PHYSICAL REVIEW D **86,** 095021 (2012)

Dark matter antibaryons from a supersymmetric hidden sector

Nikita Blinov,[1,2] David E. Morrissey,[2] Kris Sigurdson,[1] and Sean Tulin[3]

[1]*Department of Physics and Astronomy, University of British Columbia, Vancouver, British Columbia V6T 1Z1, Canada*
[2]*Theory Group, TRIUMF, 4004 Wesbrook Mall, Vancouver, British Columbia V6T 2A3, Canada*
[3]*Michigan Center for Theoretical Physics, Department of Physics, University of Michigan, Ann Arbor, Michigan 48109, USA*

(Received 25 July 2012; published 16 November 2012)

The cosmological origin of both dark and baryonic matter can be explained through a unified mechanism called hylogenesis where baryon and antibaryon numbers are divided between the visible sector and a GeV-scale hidden sector, while the Universe remains net baryon symmetric. The "missing" antibaryons, in the form of exotic hidden states, are the dark matter. We study model-building, cosmological, and phenomenological aspects of this scenario within the framework of supersymmetry, which naturally stabilizes the light hidden sector and electroweak mass scales. Inelastic dark matter scattering on visible matter destroys nucleons, and nucleon decay searches offer a novel avenue for the direct detection of the hidden antibaryonic dark matter sea.

DOI: 10.1103/PhysRevD.86.095021 PACS numbers: 98.80.Cq, 11.30.Fs, 12.60.Jv, 95.35.+d

I. INTRODUCTION

The cosmological origin of both baryonic matter [1] and dark matter [2] remain an important mystery in our understanding of the early universe. An array of astrophysical observations indicates that a fraction $\Omega_{\rm b} \approx 4.6\%$ of the energy content of the Universe is baryonic matter, while a fraction $\Omega_{\rm DM} \approx 21\%$ is dark matter (DM) [3]. The Standard Model (SM) is incapable of explaining these observations, providing no viable DM candidate, nor a successful mechanism for generating the baryon asymmetry. Cosmology therefore requires new fundamental physics beyond the SM, and it is important to find ways to detect such new physics experimentally.

The apparent coincidence between the densities of dark and baryonic matter, given by $\Omega_{\rm DM}/\Omega_{\rm b} \approx 5$, may be a clue that both originated through a unified mechanism. A wide variety of models have been proposed along these lines within the framework of asymmetric DM [4–16]; see Ref. [17] for a review. In these scenarios, DM carries a conserved global charge, and its relic abundance is determined by its initial chemical potential. Moreover, if the DM charge is related to baryon number (B), then the cosmic matter coincidence is naturally explained for $\mathcal{O}(5\ \text{GeV})$ DM mass.

In this work, we explore model-building, cosmological, and phenomenological aspects of hylogenesis ("matter genesis"), a unified mechanism for generating dark and baryonic matter simultaneously [16,18]. Hylogenesis requires new hidden sector states that are neutral under SM gauge interactions but carry nonzero B. CP-violating[1] out-of-equilibrium decays in the early universe generate a net B asymmetry among the SM quarks and an equal-and-opposite B asymmetry among the new hidden states. The Universe has zero total baryon number, but for appropriate interaction strengths and particle masses, the respective B charges in the two sectors will never equilibrate, providing an explanation for the observed asymmetry of (visible) baryons. The stable exotic particles carrying the compensating hidden antibaryon number produce the correct abundance of dark matter. Put another way, DM consists of the missing antibaryons.

The minimal hylogenesis scenario, described in Refs. [16,18], has the following three ingredients:

(1) DM consists of two states, a complex scalar Φ and Dirac fermion Ψ, each carrying $B = -1/2$.
(2) A Dirac fermion X, carrying $B = 1$, that transfers B between quarks and DM through the gauge invariant operators [19]

$$X u^c_{Ri} d^c_{Rj} d^c_{Rk}, \qquad X\Psi\Phi, \tag{1}$$

where i, j, k label generation (color indices and spinor contractions are suppressed).
(3) An additional $U(1)'$ gauge symmetry that is kinetically mixed with hypercharge and spontaneously broken near the GeV scale, producing a massive Z'.

With these ingredients, hylogenesis proceeds in three stages, which we illustrate schematically in Fig. 1:

(1) Equal (CP-symmetric) densities of X and $\bar{X}$ are created nonthermally, e.g., at the end of a moduli-dominated epoch when the Universe is reheated through moduli decay to a temperature $T_{\rm RH}$ in the range of $5\ \text{MeV} \lesssim T_{\rm RH} \lesssim 100\ \text{GeV} \ll m_X$ [20].
(2) The interactions of Eq. (1) allow X to decay to $u_{Ri} d_{R_j} d_{Rk}$ or $\bar{\Psi}\Phi^*$, and similarly for $\bar{X}$. With at least two flavors of X, these decays can violate CP leading to slightly different partial widths for X relative to $\bar{X}$, and equal-and-opposite asymmetries for visible and hidden baryons.
(3) Assuming Φ and Ψ are charged under $U(1)'$, the symmetric densities of hidden particles annihilate

[1] C is charge conjugation and P is parity.

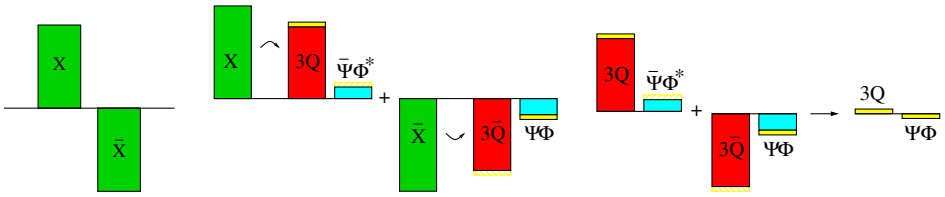

FIG. 1 (color online). The three steps of hylogenesis.

away almost completely, with $\Psi\bar{\Psi} \to Z'Z'$ and $\Phi\Phi^* \to Z'Z'$ occurring very efficiently in the hidden sector, followed by Z' decaying to SM states via kinetic mixing. The residual antibaryonic asymmetry of Φ and Ψ is asymmetric DM. Likewise, the symmetric density of visible baryons and antibaryons annihilates efficiently into SM radiation.

Both Ψ and Φ are stable provided $|m_\Psi - m_\Phi| < m_p + m_e$, and they account for the observed DM density for $m_\Psi + m_\Phi \approx 5m_p$, implying an allowed mass range $1.7 \lesssim m_{\Psi,\Phi} \lesssim 2.9$ GeV.

On the phenomenological side, hylogenesis models possess a unique experimental signature: induced nucleon decay (IND), where antibaryonic DM particles scatter inelastically on visible baryons, destroying them and producing energetic mesons. If X couples through the "neutron portal" $u_R d_R d_R$, IND produces π and η final states, while if X couples through the "hyperon portal" $u_R d_R s_R$, IND produces K final states. These signatures mimic regular nucleon decay, with effective nucleon lifetimes comparable to or shorter than existing limits; however, present nucleon decay constraints do not apply in general due to the different final state kinematics of IND. Searching for IND in nucleon decay searches, such as the Super-Kamiokande experiment [21] and future experiments [22–24], therefore offers a novel and unexplored means for discovering DM.

Although the minimal hylogenesis model described above successfully generates the cosmological baryon and DM densities, two puzzles remain. Is there a natural framework to consider DM as a quasi-degenerate scalar/fermion pair? Is there a mechanism to ensure the quantum stability of the GeV-scale masses for hidden sector scalars? Supersymmetry (SUSY) can provide answers to both questions; the DM pair (Φ, Ψ) forms a supermultiplet with $B = -1/2$, and the stability of the GeV-scale hidden sector and the (Φ, Ψ) mass splitting is ensured naturally, provided SUSY breaking is suppressed in the hidden sector compared to the visible sector.

The goal of this work is to embed hylogenesis in a supersymmetric framework of natural electroweak and hidden symmetry breaking, and to study in detail the cosmological and phenomenological consequences. In Sec. II, we present a minimal supersymmetric extension of the hylogenesis theory described above. We also address the origin of the nonrenormalizable nucleon portal operator $X u^c_{Ri} d^c_{Rj} d^c_{Rk}$. In Sec. III, we investigate the cosmological dynamics of supersymmetric hylogenesis, showing explicitly the range of masses and parameters that can explain the correct matter densities. Section IV contains a discussion of how such parameter values can arise in a natural way from various mechanisms for supersymmetry breaking. In Sec. V we investigate the phenomenology of our model, including IND signatures, collider probes, and DM direct detection. Our results are summarized in Sec. VI. In the Appendix, we also present an alternative supersymmetric model based on Higgs portal mixing.

II. SUPERSYMMETRIC HYLOGENESIS MODEL

In this section, we present an extension of the minimal supersymmetric Standard Model (MSSM) that can account for the dark matter and baryon densities through a unified mechanism of hylogenesis. In order to organize our discussion, it is useful to divide our model into three sectors, given by the superpotential terms:

$$W = W_{\rm MSSM} + W_{\rm HS} + W_{\rm trans}. \tag{2}$$

First, $W_{\rm MSSM}$ corresponds to the superpotential of the usual MSSM with weak-scale superpartners; this is the visible sector. Second, we introduce a hidden sector comprised of new states which carry B, but are uncharged under the SM gauge group, and whose interactions are described by the superpotential $W_{\rm HS}$. The third term $W_{\rm trans}$ corresponds to operators responsible for B transfer between the visible and hidden sectors. Baryon transfer operators generate equal-and-opposite B asymmetries within the two sectors, and lead to IND signatures in nucleon decay searches.

A. Hidden sector

The hidden sector of our model consists of (i) four vector-like chiral superfields carrying nonzero B, denoted $X_{1,2}$ and $Y_{1,2}$, with charge-conjugate partners $X^c_{1,2}$ and $Y^c_{1,2}$,[2] and (ii) a $U(1)'$ gauge sector, with gauge boson Z' and gauge coupling e', spontaneously broken by a vector pair of hidden Higgs supermultiplets H, H^c. Table I summarizes these exotic fields. The superpotential is given by

[2]Two species $X_{1,2}$ are required for CP-violating decays (see Sec. III), while two species $Y_{1,2}$ are needed to couple them to the gauge-singlet X fields.

TABLE I. New superfields in the hidden sector, with quantum numbers under $U(1)'$, B, and R parity. Chiral supermultiplets $X_{1,2}$, $Y_{1,2}$, H also include vector partners $X^c_{1,2}$, $Y^c_{1,2}$, H^c with opposite charge assignments (not listed).

Superfield		$U(1)'$	B	R
Hidden baryons	$X_{1,2}$	0	$+1$	-1
	Y_1	0	$-1/2$	i
	Y_2	$+1$	$-1/2$	i
Hidden $U(1)'$	H	$+1$	0	$+1$
	Z'	0	0	0

$$W_{\rm HS} = \sum_{a=1,2} \zeta_a X_a Y_1^2 + \bar{\zeta}_a X_a^c (Y_1^c)^2 + \gamma Y_1 Y_2^c H + \bar{\gamma} Y_1^c Y_2 H^c + \mu_{X_a} X_a X_a^c + \mu_{Y_a} Y_a Y_a^c + \mu_H H H^c, \tag{3}$$

which includes Yukawa-type interactions with couplings $\zeta_{1,2}$, $\bar{\zeta}_{1,2}$, γ, $\bar{\gamma}$, and vector masses $\mu_{X_{1,2}}$, $\mu_{Y_{1,2}}$, μ_H. We also assume a canonical Kähler potential for these multiplets. Note as well that we have extended R parity to a $\mathbb{Z}_4^R$ for the $Y_i^{(c)}$ multiplets. Aside from allowing the couplings listed above, this extension does not lead to any novel features in the present case, beyond those imposed by the standard R parity.

After symmetry breaking in the hidden sector, the superfields $Y_{1,2}$ and $Y^c_{1,2}$ mix to form two Dirac fermions Ψ_a ($a = 1, 2$) and four complex scalars Φ_b ($b = 1, 2, 3, 4$) with $B = -1/2$. Among these, the lightest states Ψ_1 and Φ_1 are stable DM. The fermionic mass terms for $Y_{1,2}$ are (in two-component notation)

$$\mathcal{L}_{\rm ferm} = -(Y_1^c, Y_2^c)\mathbf{M}_Y \begin{pmatrix} Y_1 \\ Y_2 \end{pmatrix} + \text{H.c.}, \qquad \mathbf{M}_Y \equiv \begin{pmatrix} \mu_{Y_1} & \bar{\gamma}\eta_c \\ \gamma\eta & \mu_{Y_2} \end{pmatrix}, \tag{4}$$

where $\eta \equiv \langle H \rangle$, $\eta_c \equiv \langle H^c \rangle$ are the hidden Higgs vacuum expectation values (vevs). This mass matrix can be diagonalized by a biunitary transformation $V^T \mathbf{M}_Y U^\dagger = \text{diag}(m_{\Psi_1}, m_{\Psi_2})$. The scalar mass terms in the basis $\tilde{Y} \equiv (\tilde{Y}_1, \tilde{Y}_2, \tilde{Y}_1^{c*}, \tilde{Y}_2^{c*})^T$ are

$$\mathcal{L}_{\rm scalar} = -\tilde{Y}^\dagger \mathbf{M}^2_{\tilde{Y}} \tilde{Y}. \tag{5}$$

The 4×4 mass matrix $\mathbf{M}^2_{\tilde{Y}}$ receives contributions from F terms from Eq. (3), D terms, and soft SUSY-breaking terms

$$-\mathcal{L}_{\rm soft} \supset m^2_{Y_1}|\tilde{Y}_1|^2 + m^2_{Y_2}|\tilde{Y}_2|^2 + m^2_{Y_1^c}|\tilde{Y}_1^c|^2 + m^2_{Y_2^c}|\tilde{Y}_2^c|^2 \tag{6}$$

$$+ (b_1 \tilde{Y}_1 \tilde{Y}_1^c + b_2 \tilde{Y}_2 \tilde{Y}_2^c + \gamma A_\gamma \tilde{Y}_1 \tilde{Y}_2^c H + \bar{\gamma} A_{\bar{\gamma}} \tilde{Y}_1^c \tilde{Y}_2 H^c + \text{H.c.}). \tag{7}$$

We have

$$\mathbf{M}^2_{\tilde{Y}} \equiv \begin{pmatrix} \mathbf{M}_Y^\dagger \mathbf{M}_Y - \boldsymbol{\delta} + \mathbf{m}^2_{\tilde{Y}} & \boldsymbol{\Delta}^\dagger \\ \boldsymbol{\Delta} & \mathbf{M}_Y \mathbf{M}_Y^\dagger + \boldsymbol{\delta} + \mathbf{m}^2_{\tilde{Y}^c} \end{pmatrix}, \qquad \boldsymbol{\Delta} \equiv \begin{pmatrix} b_1 & \gamma A_\gamma \eta \\ \bar{\gamma} A_{\bar{\gamma}} \eta_c & b_2 \end{pmatrix}, \tag{8}$$

also defining $\mathbf{m}^2_{\tilde{Y}} \equiv \text{diag}(m^2_{Y_1}, m^2_{Y_2})$, $\mathbf{m}^2_{\tilde{Y}^c} \equiv \text{diag}(m^2_{Y_1^c}, m^2_{Y_2^c})$, $\boldsymbol{\delta} \equiv e'^2(\eta_c^2 - \eta^2) \times \text{diag}(0, 1)$. The scalar mass matrix can be diagonalized by a unitary transformation $Z \mathbf{M}^2_{\tilde{Y}} Z^\dagger = \text{diag}(m^2_{\Phi_1}, m^2_{\Phi_2}, m^2_{\Phi_3}, m^2_{\Phi_4})$. Similar mass matrices arise for the X supermultiplets; for simplicity we assume that the fermion states $X_{1,2}$ and scalar states $\tilde{X}_{1,2}$, $\tilde{X}^c_{1,2}$ are all mass eigenstates.

The $U(1)'$ gauge sector consists of the Z' gauge boson, with mass $m^2_{Z'} = 2e'^2(\eta^2 + \eta_c^2)$, the $\tilde{Z}'$ gaugino, and the hidden Higgsinos $\tilde{H}$, $\tilde{H}^c$. The three neutralinos have the mass matrix

$$M = \begin{pmatrix} M' & -\sqrt{2}e'\eta & \sqrt{2}e'\eta_c \\ -\sqrt{2}e'\eta & 0 & \mu_H \\ \sqrt{2}e'\eta_c & \mu_H & 0 \end{pmatrix}, \tag{9}$$

which can be brought into a diagonal form using a unitary transformation P, such that $P^\dagger M P = \text{diag}(m_{\chi_1}, m_{\chi_2}, m_{\chi_3})$. The $U(1)'$ gauge superfield mixes kinetically with the MSSM hypercharge,

$$-\mathcal{L} \supset \frac{\kappa}{2} \int d^2\theta B^\alpha Z'_\alpha + \text{H.c.}, \tag{10}$$

where Z'_α and B_α are the $U(1)'$ and $U(1)_Y$ supersymmetric gauge field strengths, respectively, with the mixing parameter $\kappa \ll 1$.

The full particle content of the hidden sector after the spontaneous breaking of $U(1)'$ consists of the following mass eigenstates: three neutralinos χ_i; three hidden Higgs scalars h, H, A; two Dirac fermions Ψ_i; four complex scalars Φ_i; and a massive gauge boson Z'. The lightest Dirac fermion Ψ_1 and complex scalar Φ_1 are stable due to their masses and B charge assignments—they make up the dark matter. All other states either annihilate or decay into Standard Model particles as described in Sec. III.

Now that we have presented the ingredients for the hidden sector states, we make some remarks:

(i) We assume that the mass scales of the hidden sector parameters lie at the GeV scale (with the exception of the X states). For the soft terms, this can be accomplished by assuming that SUSY breaking is suppressed in the hidden sector (see Sec. IV). However, the SUSY-preserving vector mass terms present a hidden μ problem; we ignore this issue, but in principle this can be solved by introducing an additional hidden singlet analogous to the next-to-minimal supersymmetric standard model.

(ii) Since $X_{1,2}$ mediates baryon transfer between the visible and hidden sectors (described below), IND signatures are more favorable if the DM states (Φ_1, Ψ_1) are mostly aligned with the Y_1 supermultiplet. However, nonzero mixing with Y_2 is induced by SUSY breaking and hidden Higgs vevs resulting in a DM-Z' coupling that is essential for annihilation of the symmetric DM density.

(iii) We have imposed B as a global symmetry. Since gravitational effects are expected to violate global symmetries, B violation could arise through Planck-suppressed operators, potentially leading to DM particle-antiparticle oscillations that can erase the hidden baryon asymmetry [25–28]. In our SUSY framework, these effects are forbidden by the $\mathbb{Z}_4^R$ extension of R parity. For example, the $B = -1$ operators $W \sim MY_1^2$, $Y_1 Y_2 H^c$ are allowed by $U(1)'$ and can lead to DM oscillations, but they are not invariant under R parity. If $\mathbb{Z}_4^R$ descends from an anomaly-free gauge symmetry, such as $U(1)_{B-L}$ spontaneously broken by two units, it cannot be violated by gravity [29,30] and these operators are forbidden. Thus there exists a consistent embedding of $\mathbb{Z}_4^R$ in a gauge symmetry that excludes the Majorana mass terms for $Y_{1,2}$ that could erase the hidden asymmetry by oscillations.

B. Baryon transfer

The baryon number is transferred between the hidden and visible sectors through superpotential terms $W_{\rm trans}$. The hidden baryon states $X_{1,2}$ are coupled to the operator $U_i^c D_j^c D_k^c$, where U_i^c, D_j^c are the usual $SU(2)_L$-singlet quark superfields (i, j, k label generation). We focus on the case involving light quarks ($U^c \equiv U_1^c$, $D^c \equiv D_1^c$, $S^c \equiv D_2^c$), corresponding to the "hyperon portal" [19]:

$$W_{\rm trans} = \sum_{a=1,2} \frac{\lambda_a}{M} \epsilon_{\alpha\beta\gamma} X_a U_\alpha^c D_\beta^c S_\gamma^c, \tag{11}$$

with $SU(3)_C$ indices α, β, γ and nonrenormalizable couplings $\lambda_{1,2}/M$. Although hylogenesis is viable for any generational structure, Eq. (11) is the most interesting case for IND signatures. In contrast to non-SUSY hylogenesis models, the "neutron portal" coupling $X_{1,2} U^c D^c D^c$ vanishes by antisymmetry. SUSY hylogenesis therefore favors IND involving K final states, rather than π, η final states allowed in generic non-SUSY models.

The simplest possibility to generate the nonrenormalizable coupling in Eq. (11) is to introduce a vectorlike color triplet supermultiplet P with global charges $B = -2/3$ and $R = 1$. There are three cases to consider[3]:

$$W_{\rm trans} = \begin{cases} \lambda'_{1,2} X_{1,2} P_\alpha U_\alpha^c + \lambda'' \epsilon_{\alpha\beta\gamma} P_\alpha^c S_\beta^c D_\gamma^c + \mu_P P_\alpha P_\alpha^c & \text{(case I)} \\ \lambda'_{1,2} X_{1,2} P_\alpha D_\alpha^c + \lambda'' \epsilon_{\alpha\beta\gamma} P_\alpha^c U_\beta^c S_\gamma^c + \mu_P P_\alpha P_\alpha^c & \text{(case II)} \\ \lambda'_{1,2} X_{1,2} P_\alpha S_\alpha^c + \lambda'' \epsilon_{\alpha\beta\gamma} P_\alpha^c D_\beta^c U_\gamma^c + \mu_P P_\alpha P_\alpha^c & \text{(case III).} \end{cases} \tag{12}$$

The $SU(3)_C \times SU(2)_L \times U(1)_Y$ quantum numbers for P are $(3, 1, 2/3)$ for case I (up-type), and $(3, 1, -1/3)$ for cases II and III (down-type). In all cases P^c carries the opposite charges. The choice between the cases in Eq. (12) makes little difference for hylogenesis cosmology. However, the different cases affect the IND signals, manifested in the ratio of the rates of $p \to K^+$ to $n \to K^0$ channels, discussed in Sec. V.

Integrating out P and P^c at the supersymmetric level generates the superpotential operator of Eq. (11) with $\lambda_a/M \equiv \lambda'_a \lambda''/\mu_P$ together with the (higher-order) Kähler potential term (for case I, with similar operators for cases II and III):

$$K \supset \frac{|\lambda''|^2}{|\mu_P|^2} [(D^{c\dagger} D^c)(S^{c\dagger} S^c) - (S^{c\dagger} D^c)(D^{c\dagger} S^c)]. \tag{13}$$

Including supersymmetry breaking leads to additional operators. In particular, the holomorphic soft scalar coupling $b_P \tilde{P} \tilde{P}^c$ (or a squark-gaugino loop with a gaugino mass insertion) gives rise to the four-fermion operator $X u_R^c d_R^c s_R^c$ that plays a central role in IND.

III. HYLOGENESIS COSMOLOGY

We turn next to a study of the early universe dynamics of our supersymmetric model of hylogenesis. To summarize the main ingredients:

(i) We assume that the Universe is dominated at early times by a long-lived nonrelativisitic state φ (e.g., an oscillating modulus field), which decays and reheats the Universe before the onset of big bang nucleosynthesis (BBN) [20].

(ii) Nonthermal CP-symmetric densities of X_1 and $\tilde{X}_1$ states are populated through φ decays. Depending on their specific origin, the scalar or the fermion can be created preferentially [31]. CP-violating decays of X_1 and $\tilde{X}_1$ generate equal-and-opposite

[3]We consider the interactions of cases II and III separately, although in general both may arise simultaneously. The simultaneous presence of both sets of couplings leads to strangeness-violating interactions that may be constrained by flavor violation constraints that we do not consider here.

asymmetries in quarks and hidden sector baryons (Ψ, Φ), while the total baryon number is conserved.[4]

(iii) A hidden $U(1)'$ gauge sector allows for cascade decays of heavier $B = -1/2$ states (Φ_2, Ψ_2, etc.) into the lightest states $\Phi \equiv \Phi_1$ and $\Psi \equiv \Psi_1$ that are DM. Both states can be stable provided the condition $|m_\Psi - m_\Phi| < m_p + m_e$ is met. Also, the symmetric DM densities annihilate efficiently through the light Z', which decays to SM states via kinetic mixing with hypercharge.

Below, we first compute the CP asymmetries for X_1 and $\tilde{X}_1$ decays. Second, we ensure that the successful predictions of BBN are not modified by hidden sector decays into SM particles. Third, we solve the system of Boltzmann equations for hylogenesis, incorporating all of the aforementioned ingredients, to compute the baryon asymmetries. There are significant differences compared to nonsupersymmetric hylogenesis [16]; in particular, the DM masses m_Φ, m_Ψ and the ratio of Φ to Ψ states can be different, with implications for IND phenomenology.

A. *CP*-violating asymmetries

Visible and hidden B asymmetries are produced by CP violation in the partial decay widths of X_1

$$X_1 \to u_R \tilde{d}_R \tilde{s}_R + d_R \tilde{s}_R \tilde{u}_R + s_R \tilde{u}_R \tilde{d}_R, \qquad X_1 \to \bar{\Psi}_i \Phi_j^*, \tag{14}$$

due to interference between tree-level and one-loop amplitudes, shown in Fig. 2. The corresponding CP asymmetry is

$$\epsilon_X \equiv \frac{1}{\Gamma_{X_1}}[\Gamma(X_1 \to u_R \tilde{d}_R \tilde{s}_R) - \Gamma(\bar{X}_1 \to \bar{u}_R \tilde{d}_R^* \tilde{s}_R^*) + \text{perms}], \tag{15a}$$

$$= \frac{3[\mathrm{Im}(\lambda_1^* \zeta_1 \zeta_2^* \lambda_2) m_{X_1} + \mathrm{Im}(\lambda_1^* \bar{\zeta}_1^* \bar{\zeta}_2 \lambda_2) m_{X_2}] m_{X_1}^3}{64\pi^3 M^2 (m_{X_2}^2 - m_{X_1}^2)(|\zeta_1|^2 + |\bar{\zeta}_1|^2)}. \tag{15b}$$

We assume that Γ_{X_1} is dominated by the two-body decay to $\bar{\Psi}_i \Phi_j^*$ final states.[5] For $\epsilon_X > 0$, a positive net B asymmetry is generated in the visible sector. By CPT invariance, the decay rates for X_1 and $\bar{X}_1$ are equal, and so an equal-and-opposite (negative) B asymmetry is generated in the hidden sector. Additional contributions to ϵ_X from $X_1 \to u_R d_R s_R$, arising through SUSY breaking or at one-loop, may be subleading provided squark decays are kinematically available.

[4]We neglect CP-violating decays of X_2 and $\tilde{X}_2$, which in principle can also contribute to B asymmetries.

[5]In what follows, flavor indices i, j for hidden sector states are implicitly summed over in final states.

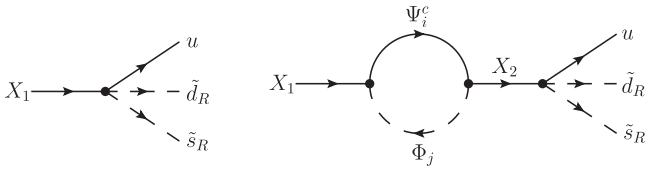

FIG. 2. Representative diagrams contributing to $X_1 \to q_i \tilde{q}_{Rj} \tilde{q}_{Rk}$ decays which are responsible for the generation of the baryon asymmetry.

The baryon asymmetry can also be generated through the decays of the scalar component of the X_1 superfield, $\tilde{X}_1$, via interference of supersymmetrizations of the diagrams in Fig. 2. In the supersymmetric limit, the CP asymmetry due to $\tilde{X}_1$ is equal to Eq. (15). However, $\tilde{X}_1$ decay can populate preferentially Ψ or Φ, due to the different hidden sector decay rates:

$$\Gamma(\tilde{X}_1 \to \Phi_i^* \Phi_j^*) = \frac{|\bar{\zeta}_1|^2}{16\pi} m_{X_1}, \qquad \Gamma(\tilde{X}_1 \to \bar{\Psi}_i \bar{\Psi}_j) = \frac{|\zeta_1|^2}{16\pi} m_{X_1}. \tag{16}$$

For X_1 decays, the primordial ratio,

$$r \equiv n_\Psi / n_\Phi, \tag{17}$$

of charge densities $n_{\Psi,\Phi}$ is equal to unity. However, $\tilde{X}_1$ decays can deviate from $r = 1$ for $|\zeta_1| \neq |\bar{\zeta}_1|$. As we discuss below, IND signals can be significantly enhanced

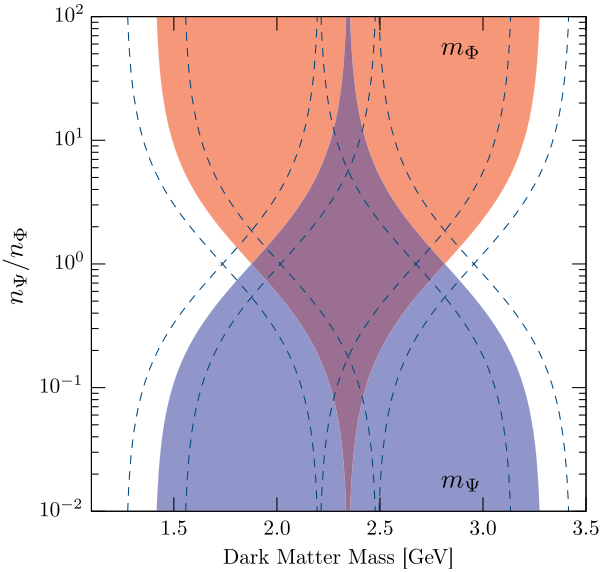

FIG. 3 (color online). Allowed masses for the scalar Φ and fermion Ψ components of dark matter. For a fixed value of n_Ψ/n_Φ, the shaded region shows the entire mass range of Ψ (blue) and Φ (red) that reproduces $\Omega_{\mathrm{DM}}/\Omega_{\mathrm{b}} \approx 5$ and satisfies the stability requirement $|m_\Psi - m_\Phi| < m_e + m_p$. Shifting $\Omega_{\mathrm{DM}}/\Omega_{\mathrm{b}}$ by $+(-)6\%$ moves the allowed region right (left), as indicated by the dashed contours.

if the heavier state is overpopulated compared to the lighter state (e.g., $r \gg 1$ for $m_\Psi > m_\Phi$).

The dark matter abundance is given by

$$\frac{\Omega_{\rm DM}}{\Omega_{\rm b}} = \frac{2(m_\Psi r + m_\Phi)}{m_p(1+r)}, \tag{18}$$

where we have neglected the contributions from the DM antiparticles. This is appropriate in the limit of completely asymmetric DM populations. The allowed DM mass window, including the uncertainty in $\Omega_{\rm DM}/\Omega_{\rm b} \approx 5$, is then

$$1.3\ {\rm GeV} \leq m_\Psi, m_\Phi \leq 3.4\ {\rm GeV}. \tag{19}$$

More specifically, Fig. 3 shows the allowed mass range for m_Ψ (blue) and m_Φ (red), for a given value of r. In the $r \to 0$ (∞) limit, only Φ (Ψ) is populated and its mass is required to be approximately $5m_p/2$ to explain the DM density; the underpopulated Ψ (Φ) state is constrained within the range of Eq. (19) by the stability condition $|m_\Psi - m_\Phi| < m_p + m_e$.

B. Decays and annihilations of SUSY states

Aside from the stable DM states Φ_1 and Ψ_1, the hidden sector contains numerous states that decay, producing additional SM radiation. These decays, listed below, must occur with a lifetime shorter than about one second to avoid conflicts with BBN predictions.

(i) The Z' gauge boson decays to SM states via kinetic mixing with the photon, requiring $\kappa \gtrsim 10^{-11}(m_{Z'}/{\rm GeV})^{-1}$ [32], while $\kappa \lesssim 10^{-3}$ is consistent with existing limits for $m_{Z'} \sim$ GeV [33,34].[6]

(ii) For the hidden Higgs states, the heavy CP-even state decays $H \to Z'Z'$, while the CP-odd state decays $A \to Z'h$, through $U(1)'$ gauge interactions. Since the lighter CP-even state h is necessarily lighter than the Z', it must decay to Standard Model fermions either via loop-suppressed processes [35] or via D-term mixing with the MSSM Higgs [36]. For h masses above the two-muon threshold, the mixing process dominates, requiring $\kappa \gtrsim 10^{-5}$.

(iii) The heavy dark states Φ_i ($i > 1$) and Ψ_2 cascade down to Φ_1 and Ψ_1 by emitting Z' and h bosons.

(iv) The hidden neutralinos can decay $\chi_i \to \Phi_1\bar{\Psi}_1$, $\Phi_1^*\Psi_1$ provided this channel is open (assumed below). If this channel is closed, then the lightest state χ_1 is stable, providing an additional DM component, and must annihilate efficiently via the t-channel process $\chi_1\chi_1 \to Z'Z'$.

In addition, the lightest supersymmetric particle within the MSSM decays to hidden states through mixing of the hidden and MSSM neutralinos induced by κ. This mixing generally has a negligible effect on the mass eigenvalues [36].

The symmetric DM densities of $\Psi_1\bar{\Psi}_1$ and $\Phi_1\Phi_1^*$ annihilate to Z' gauge bosons. In the case where DM is nearly aligned with the Y_2 multiplet, the cross sections are given by [32]

$$\begin{aligned}\langle\sigma v\rangle_{\Psi\bar{\Psi}\to Z'Z'} &= \frac{e'^4}{16\pi m_\Psi^2}\sqrt{1 - m_{Z'}^2/m_\Psi^2},\\ \langle\sigma v\rangle_{\Phi\Phi^*\to Z'Z'} &= \frac{e'^4}{16\pi m_\Phi^2}\sqrt{1 - m_{Z'}^2/m_\Phi^2}.\end{aligned} \tag{20}$$

To have $\langle\sigma v\rangle \gtrsim 3 \times 10^{-26}$ cm^3/s for efficient annihilation, we require $e' \gtrsim 0.03$ [37].

The presence of light hidden neutralinos allows for the chemical equilibration of the baryon number between Φ and Ψ. The most important process is $\Phi_1\Phi_1 \leftrightarrow \Psi_1\Psi_1$ which transfers the B asymmetry from the heavier DM state to the lighter state. This effect is phenomenologically important for IND, potentially quenching the more energetic down-scattering IND processes. The transfer arises from the supersymmetrization of the hidden gauge and Yukawa interactions, which, in the mass basis, takes the form

$$\begin{aligned}\mathcal{L} \supset \Phi_i\bar{\Psi}_j\Big[\Big(&-\sqrt{2}e' Z_{i4}^* V_{j2} P_{1k} - \gamma Z_{i1}^* V_{j2} P_{2k}\\ &- \bar{\gamma} Z_{i2}^* V_{j1} P_{3k}\Big)P_L + \Big(\sqrt{2}e' Z_{i2}^* U_{j2} P_{1k}^*\\ &- \gamma^* Z_{i4}^* U_{j1} P_{2k}^* - \bar{\gamma}^* Z_{i3}^* U_{j2}^* P_{3k}^*\Big)P_R\Big]\chi_k + {\rm H.c.}\end{aligned} \tag{21}$$

In the limit where the dark matter is mostly aligned with the Y_2 supermultiplet, the interaction simplifies to

$$\mathcal{L} \supset \sqrt{2}e'\Phi_1\bar{\Psi}_1(aP_L + bP_R)\chi_1 + {\rm H.c.}, \tag{22}$$

where $a = -\sqrt{2}e'Z_{14}^*$, $b = \sqrt{2}e'Z_{12}^*$, and χ_1 is the $U(1)'$ gaugino. Note that even if the mixing due to $U(1)'$ breaking can be neglected, the scalars $\tilde{Y}_2$ and $\tilde{Y}_2^{c*}$ will still mix via the soft b-term. For $m_\Phi \geq m_\Psi$ the s-wave contribution to the thermalized $\Phi_1\Phi_1 \to \Psi_1\Psi_1$ cross section for this interaction takes the form

$$\begin{aligned}\langle\sigma v\rangle_{\Phi\Phi\to\Psi\Psi} = &\frac{1}{8\pi(M^2 + m_\Phi^2 - m_\Psi^2)^2}\sqrt{1 - \frac{m_\Psi^2}{m_\Phi^2}}\\ &\times (2m_\Phi^2[(|a|^4 + |b|^4)m_\chi^2 + (|a|^2 + |b|^2)\\ &\times (ab^* + a^*b)m_\chi m_\Psi + 2|a|^2|b|^2 m_\Psi^2]\\ &- m_\Psi^2|(a^2 + b^2)m_\chi + 2abm_\Psi|^2).\end{aligned} \tag{23}$$

In our numerical calculations we use $a = b = e'$ for simplicity. In this case the transfer cross section reduces to

[6]We assume a stronger condition $\kappa \gtrsim 10^{-8} g_*(m_{Z'}/{\rm GeV})^{-1} \times (T_{\rm RH}/{\rm GeV})^{3/2}$ such that the hidden and visible sectors are in kinetic equilibrium at $T < T_{\rm RH}$ [32].

$$\langle\sigma v\rangle_{\Phi\Phi\to\Psi\Psi} = e'^4 \frac{(m_\chi + m_\Psi)^2}{2\pi(m_\chi^2 + m_\Phi^2 - m_\Psi^2)^2}\left(1 - \frac{m_\Psi^2}{m_\Phi^2}\right)^{3/2}. \tag{24}$$

The cross section for the reverse process $\Psi_1\Psi_1 \to \Phi_1\Phi_1$ is related to $\Phi_1\Phi_1 \to \Psi_1\Psi_1$ by the detailed balance condition

$$\langle\sigma v\rangle_{\Phi\Phi\to\Psi\Psi} = (n_\Psi^{\rm eq}/n_\Phi^{\rm eq})^2\langle\sigma v\rangle_{\Psi\Psi\to\Phi\Phi}, \tag{25}$$

where the equilibrium distributions $n_i^{\rm eq}$ are given in Eq. (34). We discuss depletion of the heavier DM state in more detail below. Before doing so, however, let us mention that the transfer process is not generic, and may be absent in other constructions. In particular, this is true of the alternate Higgs portal model presented in the Appendix.

C. Boltzmann equations

The generation of the visible and hidden B asymmetries during reheating is described by a system of Boltzmann equations:

$$\dot\rho_\varphi = -3H\rho_\varphi - \Gamma_\varphi\rho_\varphi, \tag{26a}$$

$$\dot s = -3Hs + \frac{\Gamma_\varphi}{T}\rho_\varphi, \tag{26b}$$

$$\dot n_B = -3Hn_B + (\epsilon_X\mathcal{N}_X + \epsilon_{\tilde X}\mathcal{N}_{\tilde X})\frac{\Gamma_\varphi\rho_\varphi}{m_\varphi}. \tag{26c}$$

Here, ρ_φ is the energy density of the modulus field φ, s is the entropy density, and n_B is the visible B charge density (the hidden B asymmetry is $-n_B$). Also, $\mathcal{N}_{X,\tilde X}$ is the average number of X_1 or its superpartner produced per modulus decay, while $\epsilon_{X,\tilde X}$ is the CP asymmetry from X_1, $\tilde X_1$ decay. In the supersymmetric limit $\epsilon_X = \epsilon_{\tilde X}$. The modulus decay rate Γ_φ determines the reheat temperature:

$$T_{\rm RH} = \left[\frac{45}{4\pi^3 g_*(T_{\rm RH})}\right]^{1/4}\sqrt{\Gamma_\varphi M_{\rm Pl}}. \tag{27}$$

The total modulus decay rate is given by [20,38,39]

$$\Gamma_\varphi = \frac{m_\varphi^3}{4\pi\Lambda^2}, \tag{28}$$

where we take $\Lambda = 2.43\times10^{18}$ GeV to be the reduced Planck constant. Along with the Friedmann equation $H^2 = (8\pi G/3)(\rho_\varphi + \rho_r)$, where $\rho_r = (\pi^2/30)g_*T^4$, Eq. (26) forms a closed set and can be solved using the method of Refs. [40,41]. Here g_* is the energy density number of relativistic degrees of freedom. Instead of entropy, one can also solve for radiation density. We take $m_\varphi = 2000$ TeV (corresponding to $T_{\rm RH} \approx 270$ MeV), $\mathcal{N}_X = \mathcal{N}_{\tilde X} = 1$, and $\epsilon_X = \epsilon_{\tilde X} = 3.68\times10^{-4}$. This decay asymmetry can be generated, for example, by taking $|\lambda_a| \approx 1$, $|\zeta_a| \approx 0.1$,[7]

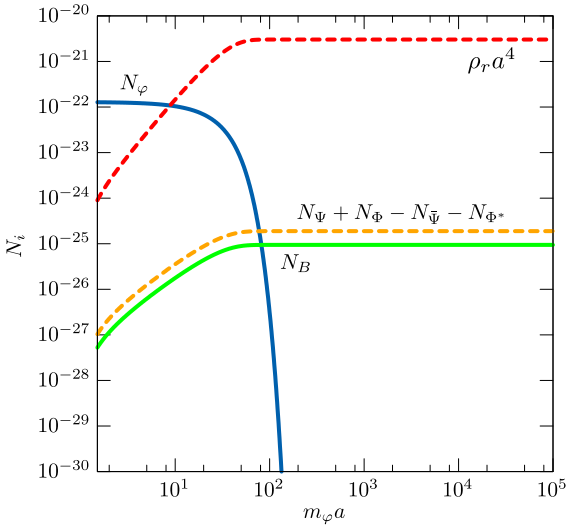

FIG. 4 (color online). Solutions to the reheating equations, (26a)–(26c), and DM production, described by Eq. (29). Here $N_\varphi = \rho_\varphi a^3/m_\varphi$ and $N_i = n_i a^3$ for $i = B$, Ψ, Φ, $\bar\Psi$, Φ^*.

the maximal CP-violating phase and $M \approx m_{X_1} \approx m_{X_2}/3 \approx 1$ TeV. These parameters reproduce the observed baryon asymmetry $\eta_B = n_B/s \approx 8.9\times10^{-11}$. Numerical solutions to the reheating equations for these parameters are shown in Fig. 4. The modulus field φ decays into radiation and the heavy states X, which immediately decay asymmetrically in the visible and hidden sectors, generating the baryon asymmetry and the dark matter abundance.

The production of dark matter and its dynamics are described by a system of four Boltzmann equations for Ψ_1, Φ_1 and their antiparticles[8] which take the form

$$\dot n_i = -3Hn_i + C_i + (\mathcal{N}_{i,X}\mathcal{N}_X + \mathcal{N}_{i,\tilde X}\mathcal{N}_{\tilde X})\frac{\Gamma_\varphi\rho_\varphi}{m_\varphi}, \tag{29}$$

for $i = \Psi_1$, $\bar\Psi_1$, Φ_1, Φ_1^*. Here $\mathcal{N}_{i,X}$ is the average number of species i produced per X decay. For $i = \Psi$ (we drop the subscript 1 from hereon) we have

$$\mathcal{N}_\Psi \equiv \mathcal{N}_{\Psi,X} + \mathcal{N}_{\Psi,\tilde X} = \frac{\Gamma(\tilde X \to \Psi\Phi) + 2\Gamma(\tilde X^* \to \Psi\Psi)}{\Gamma_X}. \tag{30}$$

Similar definitions hold for $\bar\Psi$, Φ, and Φ^*, so that

$$\mathcal{N}_\Psi + \mathcal{N}_\Phi - \mathcal{N}_{\bar\Psi} - \mathcal{N}_{\Phi^*} = 2\epsilon_X + 2\epsilon_{\tilde X}. \tag{31}$$

The last term on the right-hand side of Eq. (29) describes the production of the species i through modulus decay into

[7]The magnitude of the coupling constants is chosen to be consistent with hidden sector SUSY breaking as discussed in Sec. IV.

[8]We assume that the heavier dark states Ψ_2 and Φ_i, $i > 1$, decay to Ψ_1 and Φ_1 sufficiently fast.

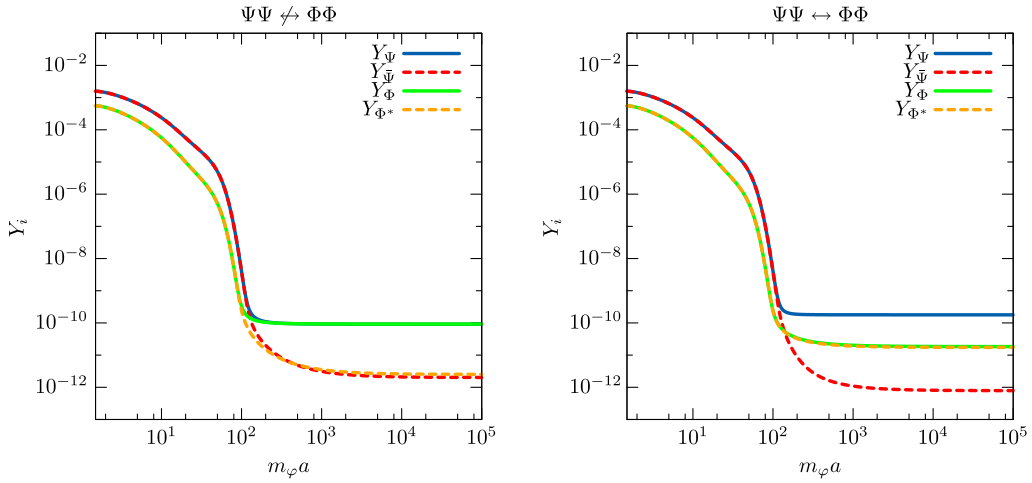

FIG. 5 (color online). Solution to the Boltzmann equations for the yields $Y_i = n_i/s$ as a function of the scale factor a. The plot on the left shows the evolution for the case when the transfer reaction $\Phi\Phi \leftrightarrow \Psi\Psi$ is turned off, while the plot on the right shows the outcome when it is active. The transfer drives the dark matter population into a lighter state, Ψ in this case. The DM (anti-DM) abundance is indicated by solid (dashed) lines, with dark (light) lines referring to the fermion (scalar) component. The parameters used are described in the text.

X which promptly decays into i. The quadratic collision terms C_i describe the particle-antiparticle annihilations as well as the transfer reaction $\Psi\Psi \leftrightarrow \Phi\Phi$, required by supersymmetry. The collision terms for $i = \Psi, \Phi$ are

$$C_\Psi = -\langle\sigma v\rangle_{\Psi\bar\Psi\to Z'Z'}[n_\Psi n_{\bar\Psi} - (n_\Psi^{\rm eq})^2] - \langle\sigma v\rangle_{\Psi\Psi\to\Phi\Phi}[n_\Psi^2 - (n_\Psi^{\rm eq}/n_\Phi^{\rm eq})^2 n_\Phi^2], \quad (32)$$

$$C_\Phi = -\langle\sigma v\rangle_{\Phi\Phi^*\to Z'Z'}[n_\Phi n_{\Phi^*} - (n_\Phi^{\rm eq})^2] - \langle\sigma v\rangle_{\Phi\Phi\to\Psi\Psi}[n_\Phi^2 - (n_\Phi^{\rm eq}/n_\Psi^{\rm eq})^2 n_\Psi^2], \quad (33)$$

where

$$n_i^{\rm eq} = \frac{g_i}{2\pi^2} T m_i^2 K_2(m_i/T) \quad (34)$$

is the Maxwell-Boltzmann equilibrium number density for a particle of mass m_i with g_i internal degrees of freedom. The collision terms for the antiparticles are identical, with the replacements $\Psi \to \bar\Psi$ and $\Phi \to \Phi^*$.

The solutions to the Boltzmann equations for the yields $Y_i = n_i/s$ are shown in Fig. 5 for $m_\Psi = 1.9$ GeV, $m_\Phi = 2.2$ GeV, $m_\chi = 5$ GeV, $e' = 0.05$. We consider two cases. In the plot on the left, we show the limit where $\langle\sigma v\rangle_{\Phi\Phi\leftrightarrow\Psi\Psi} = 0$; this can occur when the rate is mixing suppressed, for a heavy gaugino, or within models with alternative symmetric annihilation mechanisms (see the Appendix). With the transfer turned off, the scalar and fermion DM sectors are decoupled. The resulting DM abundances are determined by the X and $\tilde X$ decay asymmetries. In this limit, the dark sector reduces to two independent copies of the standard asymmetric DM scenario. We show the case where Ψ and Φ are populated equally by the $\tilde X$ decays, but, in general, the asymmetries can be different for the scalar and fermion DM, as discussed in Sec. III A.

In the plot on the right we show the result when the transfer is efficient, driving the dark matter population into the lighter state Ψ. Since the asymmetry is also transferred into the lighter state, the $\Psi\bar\Psi$ annihilation rate is enhanced, resulting in a highly asymmetric final abundance. The heavier state, on the other hand, freezes out with nearly equal abundances of particle and antiparticle, which are about an order of magnitude smaller than that of Ψ. The transfer reaction does not affect the production of the net hidden sector baryon number $n_\Psi + n_\Phi - n_{\bar\Psi} - n_{\Phi^*}$. Its evolution is shown in Fig. 4. Note that

$$n_\Psi + n_\Phi - n_{\bar\Psi} - n_{\Phi^*} = 2n_B \quad (35)$$

as required by B conservation in hylogenesis.

The ratio of the abundances of Ψ to Φ is important for IND. We study the effect of varying the mass splitting $\Delta m = m_\Phi - m_\Psi$ and the gaugino mass on n_Ψ/n_Φ in Fig. 6. For each point in the parameter space, we solve the reheating and DM production equations and plot the final value of n_Ψ/n_Φ. The reheating temperature, asymmetry, and gauge coupling strength are the same as for Fig. 5. Setting the DM abundance to the observed value fixes m_Ψ. Light gauginos and large DM mass splittings make the transfer more efficient, increasing the abundance of the lighter state relative to the heavier one. For small Δm or heavy m_χ the transfer rate is suppressed.

If the symmetric density does not annihilate efficiently, residual annihilations during the cosmic microwave background (CMB) era can inject enough energy to alter the power spectrum. The WMAP7 constraint on the annihilation rate for Dirac fermions or complex scalars is given by [42]

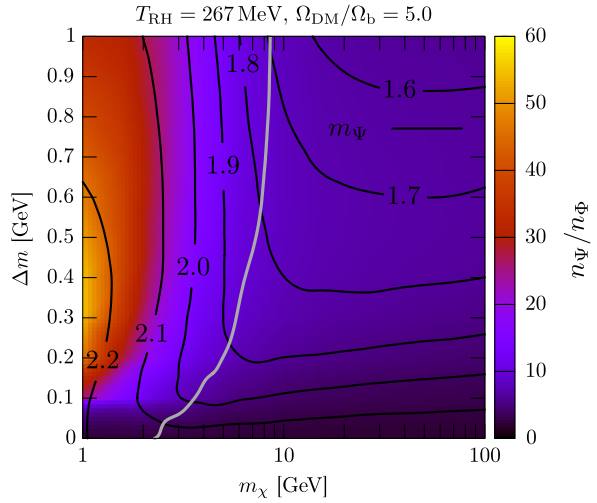

FIG. 6 (color online). The ratio n_Ψ/n_Φ for the allowed range of mass splittings $\Delta m = m_\Phi - m_\Psi$ and relevant values of the hidden gaugino mass m_χ. At each point in the plane the DM abundance is fixed to be $\Omega_{\rm DM}/\Omega_{\rm b} = 5.0$. Contours of constant m_Ψ (in GeV) are also shown. The gray contour shows the CMB constraint for DM annihilations from Ref. [42]. Points to the right of this line are excluded.

$$2\frac{\Omega_i\Omega_{\bar{i}}}{\Omega_{\rm DM}^2}\frac{f\langle\sigma v\rangle}{m_i} < \frac{2.42\times10^{-27}\ {\rm cm}^3/{\rm s}}{\rm GeV}, \tag{36}$$

where $i = \Psi$, Φ, and $\Omega_i/\Omega_{\rm DM}$ is the fraction of total DM abundance in species i. This constraint is shown in Fig. 6 by the gray line (parameter space to the right is excluded). For the parameters we have chosen, symmetric annihilation is only marginally efficient, and transfer processes through the light gaugino help achieve efficient annihilation (hence, the large m_χ region is excluded). For larger gauge coupling $e' = 0.1$, symmetric annihilation is much more efficient, and CMB constraints are evaded in the entire parameter region in Fig. 6.

Finally, let us mention that we have not included any baryon washout processes in our Boltzmann equations. For $T_{RH} \ll m_{X_1}, m_{\tilde{q}}$, the only such processes that are allowed kinematically are $\Psi\Phi \leftrightarrow 3\bar{q}$ and the corresponding crossed diagrams. These transitions require the exchanges of massive intermediate P and X states to occur. These processes are therefore well described by effective operators of the kind

$$\mathcal{L} \sim \frac{1}{\Lambda_{\rm IND}^3} uds\Psi\Phi, \tag{37}$$

where the scale $\Lambda_{\rm IND}$ is defined in Sec. V [see Eq. (52)] and the order of fermion contractions depends on which UV completion is used in Eq. (12). We find that the corresponding cross sections are safely smaller than the stringent limits found in Ref. [43] provided m_X, $m_P \gtrsim 300$ GeV. For example, we can estimate the cross section for $\Psi\Phi \leftrightarrow 3\bar{q}$ as

$$\langle\sigma v\rangle \sim \left(\frac{1}{4\pi}\right)^3 \frac{m_{\Psi_1}^4}{\Lambda_{\rm IND}^6} = (4\times10^{-21}\ {\rm GeV}^{-2})\left(\frac{1{\rm TeV}}{\Lambda_{\rm IND}}\right)^6\left(\frac{m_{\Psi_1}}{3\ {\rm GeV}}\right)^4. \tag{38}$$

The authors of Ref. [43] found that washout is negligible for

$$m_{\rm DM}\langle\sigma v\rangle \lesssim 10^{-18}\ {\rm GeV}^{-1}, \tag{39}$$

which is easily satisfied by Eq. (38). Even if these processes were important, the X_1 decay asymmetry can be adjusted to compensate, as long as the couplings satisfy the conditions imposed by SUSY breaking discussed in the next section. Thus, our omission of baryon washout effects is justified.

IV. SUPERSYMMETRY BREAKING

Our model for asymmetric antibaryonic dark matter typically requires light hidden scalars with masses of a few GeV to obtain an acceptable dark matter abundance. For such masses to be technically natural, the size of soft supersymmetry breaking felt by the light states should also be near the GeV scale. This is much smaller than the minimal scale of supersymmetry breaking felt in the MSSM sector, which must be close to or above the TeV scale to be consistent with current experimental bounds.

Such a hierarchy between visible and hidden sector soft terms can arise if the hidden sector feels supersymmetry breaking more weakly than the visible. We examine here the necessary conditions for this to be the case based on the interactions required for hylogenesis. We also discuss a few specific mechanisms of supersymmetry breaking that can give rise to the required spectrum. Motivated by the desire for large moduli masses, which are frequently on the same order as the gravitino mass, we pay particular attention to anomaly mediation.

A. Minimal transmission of supersymmetry breaking

The interactions we have put forward in Sec. II will transmit supersymmetry breaking from the MSSM to the hidden sector. Thus, a minimal requirement for small hidden-sector soft terms is that these interactions do not themselves create overly large hidden soft masses. We begin by studying these effects.

The states that we wish to remain light derive from the $Y_{1,2}^{(c)}$ and $H^{(c)}$ chiral multiplets. These multiplets do not couple directly to the MSSM, but they are connected indirectly by their interactions with the $X^{(c)}$ states and $U(1)' - U(1)_Y$ gauge kinetic mixing. Thus, the $X^{(c)}$ multiplets and the gauge kinetic mixing will act as mediators to the hidden states.

Beginning with the X multiplets, they will feel supersymmetry breaking from their direct couplings to the quarks and the triplet $P^{(c)}$ given in Eq. (12). The transmission of supersymmetry breaking can be seen in the renormalization group (RG) equations of the soft scalar squared masses of $X_a^{(c)}$ and $P^{(c)}$ (assuming interactions as in case I):

$$\begin{aligned}
(4\pi)^2\frac{dm_{X_a}^2}{dt} &= 6|\lambda'_a|^2(m_{X_a}^2 + m_{U^c}^2 + m_P^2 + |A_{\lambda'_a}|^2) + 4|\zeta_a|^2(m_{X_a}^2 + 2m_Y^2 + |A_{\zeta_a}|^2),\\
(4\pi)^2\frac{dm_{X_a^c}^2}{dt} &= 4|\bar{\zeta}_a|^2(m_{X_a^c}^2 + 2m_{Y^c}^2 + |A_{\bar{\zeta}_a}|^2),\\
(4\pi)^2\frac{dm_P^2}{dt} &= \sum_a 2|\lambda'_a|^2(m_{X_a}^2 + m_{U^c}^2 + m_P^2) - \frac{32}{3}g_3^2|M_3|^2 + \ldots,\\
(4\pi)^2\frac{dm_{P^c}^2}{dt} &= 4|\lambda''|^2(m_{S^c}^2 + m_{D^c}^2 + m_{P^c}^2) - \frac{32}{3}g_3^2|M_3|^2 + \ldots,
\end{aligned} \tag{40}$$

where the A_i are trilinear soft terms corresponding to superpotential operators, and we have dropped subleading hypercharge contributions for $P^{(c)}$. We see that P and P^c will typically obtain full-strength (TeV) soft masses from their direct coupling to the gluon multiplet, and these will be passed on to X in the course of RG evolution. Recall as well that $\lambda'_{1,2}$ and λ'' must both be reasonably large for hylogenesis to work.

Turning next to the Y multiplets, we find for the Y_1

$$\begin{aligned}
(4\pi)^2\frac{dm_{Y_1}^2}{dt} &= \sum_a 8|\zeta_a|^2(m_{X_a}^2 + m_{Y_1}^2 + |A_{\zeta_a}|^2) + 2|\gamma|^2(m_H^2 + m_{Y_1}^2 + m_{Y_2^c}^2 + |A_\gamma|^2),\\
(4\pi)^2\frac{dm_{Y_1^c}^2}{dt} &= \sum_a 8|\bar{\zeta}_a|^2(m_{X_a^c}^2 + m_{Y_1^c}^2 + |A_{\bar{\zeta}_a}|^2) + 2|\bar{\gamma}|^2(m_{H^c}^2 + m_{Y_1^c}^2 + m_{Y_2}^2 + |A_{\bar{\gamma}}|^2).
\end{aligned} \tag{41}$$

The Y_2 multiplets are also charged under the $U(1)'$ hidden gauge symmetry, which mixes kinetically with hypercharge with strength κ. This leads to additional contributions to the running [44–46]. At leading nontrivial order in κ, we have

$$\begin{aligned}
(4\pi)^2\frac{dm_{Y_2}^2}{dt} &= 2|\bar{\gamma}|^2(m_{H^c}^2 + m_{Y_1^c}^2 + m_{Y_2}^2 + |A_{\bar{\gamma}}|^2) - 8e'^2(|M'|^2 + \kappa^2|M_1|^2) + 2e'^2S_{Z'} - 2\kappa\sqrt{\frac{3}{5}}g_1e'S_Y,\\
(4\pi)^2\frac{dm_{Y_2^c}^2}{dt} &= 2|\gamma|^2(m_H^2 + m_{Y_1}^2 + m_{Y_2^c}^2 + |A_\gamma|^2) - 8e'^2(|M'|^2 + \kappa^2|M_1|^2) - 2e'^2S_{Z'} + 2\kappa\sqrt{\frac{3}{5}}g_1e'S_Y,
\end{aligned} \tag{42}$$

where $S_{Z'} = \mathrm{tr}(Q'm^2)$, $S_Y = \mathrm{tr}(Ym^2)$, $g_1 = \sqrt{5/3}g_Y$, and M_1 is the hypercharge gaugino (bino) mass. The RG equations for the soft mass of H (H^c) have the same form as for Y_2^c (Y_2) but with signs of the last two "S" terms reversed.

In addition to these RG contributions, there is D-term mixing between hypercharge and $U(1)'$. After electroweak symmetry breaking in the MSSM sector, this generates an effective Fayet-Iliopoulos [44,45] term in the hidden sector of the form

$$V \supset \frac{e'^2}{2}(|H|^2 + |Y_2|^2 - |H^c|^2 - |Y_2^c|^2 - \xi_{FI})^2, \tag{43}$$

with $\xi_{FI} = -\kappa(g_Y/2e')v^2\cos(2\beta)$, where $v \approx 174$ GeV and $\tan\beta$ is the ratio of MSSM Higgs vevs. This term can be absorbed by shifting the hidden-sector soft masses by $m_i^2 \to (m_i^2 - Q'_i\xi_{FI})$.

The RG equations we have presented here are valid down to the scale m_{soft} where the MSSM [and X and $P^{(c)}$ if their supersymmetric masses are near m_{soft}] states should be integrated out. This will generate additional threshold corrections to the hidden-sector soft masses. However, these lack the logarithmic enhancement of the RG contributions and are typically subleading. Thus, putting these pieces together we can make estimates for the minimal natural values of the soft terms in the hidden sector. In terms of $m_{\mathrm{soft}} \sim M_3 \sim$ TeV and $\Delta t = \ln(\Lambda_*/m_{\mathrm{soft}})$ (where Λ_* is the scale of supersymmetry-breaking mediation), we find

$$m_{P^{(c)}} \gtrsim m_{\mathrm{soft}}, \tag{44}$$

$$m_{X^{(c)}} \gtrsim |\lambda'|m_{\mathrm{soft}}\left(\frac{\sqrt{\Delta t}}{6}\right), \tag{45}$$

$$m_{Y_1^{(c)}} \gtrsim |\zeta\lambda'| m_{\rm soft}\left(\frac{\sqrt{\Delta t}}{6}\right)^2, \tag{46}$$

$$m_{Y_2^{(c)}}, m_{H^{(c)}} \gtrsim \max\left\{|\gamma\zeta\lambda'| m_{\rm soft}\left(\frac{\sqrt{\Delta t}}{6}\right)^{3/2}, \kappa M_1\left(\frac{\sqrt{\Delta t}}{6}\right), \sqrt{\frac{\kappa g_Y}{2e'}}v\right\}. \tag{47}$$

Note that $\sqrt{\Delta t} \approx 6$ for $\Lambda_* = M_{\rm Pl}$. We see that the soft masses of the Y_2 and H multiplets can be naturally suppressed relative to the MSSM for relatively small couplings. For example, choosing $\gamma = e' = 0.05$, $\lambda'_1 = 1$, $\kappa \sim 10^{-4}$, and $\zeta = 0.1$ yields soft masses for the $Y_2^{(c)}$ and $H^{(c)}$ multiplets below a few GeV. Therefore the direct coupling of the MSSM to the hidden sector need not induce overly large supersymmetry breaking in the hidden sector.

B. Mediation mechanisms

We consider next a few specific mechanisms to mediate supersymmetry breaking to the MSSM and the hidden sector that will produce a mass hierarchy between the two sectors. Motivated by our desire for large moduli masses, which in supergravity constructions are frequently related closely to the gravitino mass [47,48], the mechanism we will focus on primarily is anomaly mediation. However, we will also describe a second example using gauge mediation with mediators charged only under the SM gauge groups.

With anomaly mediated supersymmetry breaking (AMSB) [49,50], the leading-order gaugino mass in the hidden sector is

$$M' = \frac{b' e'^2}{(4\pi)^2} m_{3/2}, \tag{48}$$

where $b' = -4$ is the one-loop $U(1)'$ beta function coefficient. A similar expression applies to the MSSM gaugino soft masses, but with $e'^2 b'$ replaced by the corresponding factor. Based on this comparison, we see that a much lighter hidden gaugino will arise for small values of the hidden gauge coupling [51]. For example, with MSSM gaugino masses in the range of a few hundred GeV, the hidden gaugino mass will be a few GeV for $e'/g_{\rm SM} \sim 0.1$, corresponding to $e' \sim 0.05$.

The hidden-sector scalar soft masses will also be parametrically smaller than those of the MSSM if the corresponding Yukawa couplings are smaller as well. The explicit AMSB expressions for Y_1 and Y_2^c are

$$\begin{aligned} m^2_{Y_1} &= \frac{m^2_{3/2}}{(4\pi)^4}\Big[\gamma^2(3\gamma^2 - 4e'^2) + 6\gamma^2\sum_a \zeta_a^2 \\ &\quad + 6\sum_a \zeta_a^2\lambda_a'^2 + 4\sum_{a,b}\zeta_a^2\zeta_b^2(2+\delta_{ab})\Big], \\ m^2_{Y_2^c} &= \frac{m^2_{3/2}}{(4\pi)^4}\Big[\gamma^2(3\gamma^2 - 4e'^2) + 2\gamma^2\sum_a \zeta_a^2 - 16e'^2\Big]. \end{aligned} \tag{49}$$

We also have $m^2_H = m^2_{Y_2^c}$, while $m^2_{H^c} = m^2_{Y_2}$ are given by the same expressions with $\gamma \to \bar\gamma$ and $\zeta_a \to \bar\zeta_a$. The latter point also applies to $m^2_{Y_1^c}$ relative to $m^2_{Y_1}$ but with $\lambda'_a \to 0$ as well. Thus, we find GeV-scale soft masses for $Y_2^{(c)}$ and $H^{(c)}$ (and TeV-scale MSSM soft masses) for the fiducial values $\zeta_a \sim 0.1$, $\gamma \sim e' \sim 0.05$, and $m_{3/2} \sim 100$ TeV. Note that in these expressions we have neglected kinetic mixing effects which are negligible for $\kappa < 10^{-3} \ll e'/g_1$, as we assume here.

The result of Eq. (49) shows that the AMSB scalar squared masses can be positive or negative, depending on the relative sizes of the gauge and Yukawa couplings. This feature creates a severe problem in the MSSM where minimal AMSB produces tachyonic sleptons. We assume that one of the many proposed solutions to this problem corrects the MSSM soft masses without significantly altering the soft masses in the hidden sector [52,53]. In contrast to the MSSM, negative scalar soft squared masses need not be a problem in the hidden sector due to the presence of supersymmetric mass terms for all the multiplets. In particular, the supersymmetric mass terms we have included in Eqs. (3) and (12) for the vector-like hidden multiplets can generally be chosen so that only the H and H^c multiplets develop vevs.

Let us mention, however, that supersymmetric mass terms are problematic in AMSB. In particular, a fundamental supersymmetric mass term M_i will give rise to a corresponding holomorphic bilinear soft "b_i" term of size $b_i \sim M_i m_{3/2}$. If $b_i \gg m^2_{\rm soft}, |M_i|^2$, such a term will destabilize the scalar potential. To avoid this, we must assume that the supersymmetric mass terms we have written in Eqs. (3) and (12) are generated in some other way, such as from the vev of a singlet field.[9] A full construction of such a remedy lies beyond the scope of the present work, but we expect that it can be achieved in analogy to the many similar constructions addressing the corresponding μ-$B\mu$ problem within the MSSM [52,53] or beyond [51].

A second option for the mediation of supersymmetry breaking that preserves the MSSM-hidden mass hierarchy is gauge mediation by messengers charged only under the SM gauge groups [44,45]. The soft masses generated in the hidden sector in this case can be deduced from the RG equations, up to boundary terms at the messenger scale on the order of $\kappa m_{\rm soft}$, which are safely small. Unfortunately, the $U(1)'$ gaugino mass generated in this scenario only appears at very high loop order, and tends to be unacceptably small [45]. This can be resolved if there are additional gravity-mediated contributions to all the soft masses on the order of a few GeV. The gravitino mass in this case will be

[9]Note that we could have $|\mu_P|$, $|\mu_X| \gg m_{3/2}$ without any problems. In this case, the threshold corrections to the light soft masses from integrating out the heavy multiplets precisely cancel their leading contributions from RG, leading to a zero net one-loop AMSB contribution.

on the same order as the hidden states. If it is slightly lighter, it may permit the decay $\Psi_1 \to \psi_{3/2} + \Phi_1$ (for $m_{\Psi_1} > m_{3/2} + m_{\Phi_1}$).

V. PHENOMENOLOGY

A. Induced nucleon decay

Dark matter provides a hidden reservoir of antibaryons. Although baryon transfer interactions are weak enough that visible baryons and hidden antibaryons are kept out of chemical equilibrium today, they are strong enough to give experimentally detectable signatures of DM-induced nucleon destruction. In these events, a DM particle scatters inelastically on a nucleon $N = p$, n, producing a DM antiparticle and mesons. For SUSY models, the simplest IND events are those involving a single kaon,

$$\Psi N \to \Phi^* K, \qquad \Phi N \to \bar{\Psi} K. \tag{50}$$

We consider only the lightest DM states $\Psi \equiv \Psi_1$ and $\Phi \equiv \Phi_1$; the heavier states are not kinematically accessible provided their mass gap is larger than $(m_N - m_K) \approx 400$ MeV. Both down scattering and up scattering can occur (defined as whether the heavier DM state is in the initial or final state, respectively), but up scattering is kinematically forbidden for $|m_\Psi - m_\Phi| < m_N - m_K$.

Assuming the hidden states are not observed, IND events mimic standard nucleon decay events $N \to K\nu$, with an unobserved neutrino ν (or antineutrino $\bar{\nu}$). Nucleon decay searches by the Super-Kamiokande experiment have placed strong limits on the N lifetime τ for these modes [21]:

$$\begin{aligned} \tau(p \to K^+ \nu) &> 2.3 \times 10^{33} \text{ yr}, \\ \tau(n \to K_S^0 \nu) &> 2.6 \times 10^{32} \text{ yr}. \end{aligned} \tag{51}$$

However, these bounds do not in general apply to IND, due to the different kinematics. For $N \to K\nu$, the K has momentum $p_K \approx 340$ MeV. IND events are typically more energetic: $680 \lesssim p_K \lesssim 1400$ MeV for down scattering, and $p_K \lesssim 680$ MeV for up scattering (if allowed).[10] The Super-Kamiokande analysis assumes that for $p \to K^+$, K^+ is emitted below the Čerenkov threshold in water, corresponding to $p_K \lesssim 550$ MeV; for $p \to K_S^0$, the K_S^0 is emitted with $200 < p_K < 500$ MeV. Therefore, IND is largely unconstrained by standard nucleon decay searches. The limits in Eq. (51) only constrain up-scattering IND in a subset of parameter space, whereas down scattering provides typically the dominant contribution to the total IND rate [18].

[10]For fixed DM masses, IND is either bichromatic or monochromatic, depending on whether up scattering is allowed or not; the range in p_K corresponds to the allowed mass range $1.4 \lesssim m_{\Phi,\Psi} \lesssim 3.3$ GeV. If other hidden states $\Psi_{a\geq 2}$ and $\Phi_{b\geq 2}$ are kinematically accessible, the IND spectrum can have additional spectral lines.

Next, we compute the IND rates within our supersymmetric model, starting from the baryon transfer superpotential in Eq. (12). The vector-like squarks $\tilde{P}$, $\tilde{P}^c$ mix through the SUSY-breaking term $\mathcal{L}_{\text{soft}} \supset b_P \tilde{P}\tilde{P}^c$ to generate the mass eigenstates $\tilde{P}_{1,2}$, with masses $m_{\tilde{P}_{1,2}}$. The leading contribution to IND arises from the tree-level $\tilde{P}_{1,2}$ exchange, shown in Fig. 7, giving (in two-component notation)

$$\begin{aligned} L_{\text{eff}} &= \frac{1}{\Lambda_{\text{IND}}^3} \times \begin{cases} \epsilon_{\alpha\beta\gamma}(d_R^\alpha s_R^\beta)(u_R^\gamma \Psi_R)\Phi & \text{(case I)} \\ \epsilon_{\alpha\beta\gamma}(s_R^\alpha u_R^\beta)(d_R^\gamma \Psi_R)\Phi & \text{(case II)} \\ \epsilon_{\alpha\beta\gamma}(u_R^\alpha d_R^\beta)(s_R^\gamma \Psi_R)\Phi & \text{(case III)}, \end{cases} \\ \frac{1}{\Lambda_{\text{IND}}^3} &\equiv \sum_{a=1,2} \frac{2\tilde{\zeta}_a^* Z_{31} V_{11}^* b_P \lambda_a' \lambda'}{m_{\tilde{P}_1}^2 m_{\tilde{P}_2}^2 m_{X_a}}. \end{aligned} \tag{52}$$

Here, we have neglected higher derivative terms, and Λ_{IND} characterizes the IND mass scale. The different cases, corresponding to different baryon transfer interactions in Eq. (12), lead to different fermion contractions.

The effective IND rate for nucleon $N = p$, n is

$$\Gamma(N \to K) = n_\Psi (\sigma v)_{\text{IND}}^{N\Psi \to K\Phi^\dagger} + n_\Phi (\sigma v)_{\text{IND}}^{N\Phi \to K\bar{\Psi}}, \tag{53}$$

where $n_{\Psi,\Phi}$ are the local DM number densities and $(\sigma v)_{\text{IND}}$ is the IND cross section. The IND lifetime can be expressed as

$$\begin{aligned} \tau(N \to K) &= \frac{1}{\Gamma(N \to K)} \\ &= \frac{(1+r)(\Omega_{\text{DM}}/\Omega_{\text{b}}) m_p}{2\rho_{\text{DM}}[r(\sigma v)_{\text{IND}}^{N\Psi \to K\Phi^\dagger} + (\sigma v)_{\text{IND}}^{N\Phi \to K\bar{\Psi}}]}, \end{aligned} \tag{54}$$

with local DM mass density $\rho_{\text{DM}} = m_\Psi n_\Psi + m_\Phi n_\Phi$, and assuming the local ratio $r \equiv n_\Psi / n_\Phi$ is the same as over cosmological scales. The IND cross section is estimated as

$$(\sigma v)_{\text{IND}} \approx \frac{m_{\text{QCD}}^4}{16\pi \Lambda_{\text{IND}}^6} \approx 10^{-39} \text{ cm}^3/\text{s} \times \left(\frac{\Lambda_{\text{IND}}}{1 \text{ TeV}}\right)^{-6}, \tag{55}$$

with QCD scale $m_{\text{QCD}} \approx 1$ GeV.[11] For $r \sim \mathcal{O}(1)$, the IND lifetime is

$$\begin{aligned} &\tau(N \to K) \\ &\quad \approx 10^{32} \text{ yr} \times \left(\frac{(\sigma v)_{\text{IND}}}{10^{-39} \text{ cm/s}}\right)^{-1} \left(\frac{\rho_{\text{DM}}}{0.3 \text{ GeV/cm}^3}\right)^{-1}, \end{aligned} \tag{56}$$

which is exactly in the potential discovery range of existing nucleon decay searches, provided the baryon transfer scale Λ_{IND} is set by the weak scale.

[11]The cross section $(\sigma v)_{\text{IND}}$ also depends on the DM masses $m_{\Psi,\Phi}$, which for the purposes of dimensional analysis are comparable to m_{QCD}.

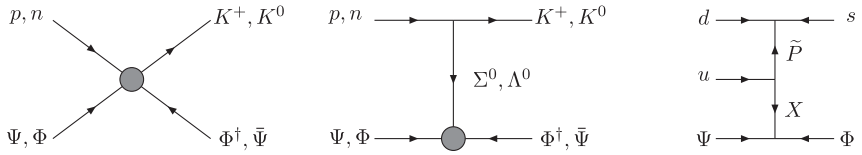

FIG. 7. IND processes at leading order in chiral effective theory (left, center). The gray dot shows the effective B transfer operator, generated by the $\tilde{P}$, X exchange in our model (right).

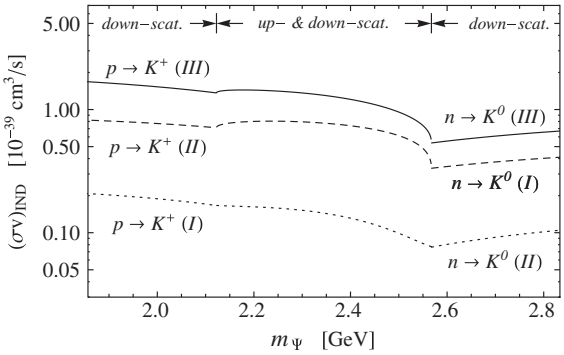

FIG. 8. Total IND cross section $(\sigma v)_{\rm IND} = (\sigma v)^{N\Psi\to K\Phi^*}_{\rm IND} + (\sigma v)^{N\Phi\to K\Psi}_{\rm IND}$ over allowed range for m_Ψ, with $m_\Phi = (\Omega_{\rm DM}/\Omega_{\rm b})m_p - m_\Psi \approx 5m_p - m_\Psi$. The effective baryon transfer mass scale is $\Lambda_{\rm IND} = 1$ TeV. Cases I, II, and III correspond to different baryon transfer models considered in Eqs. (12) and (52).

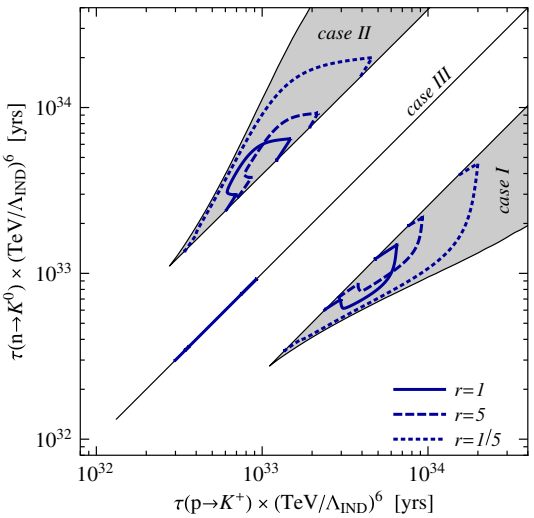

FIG. 9 (color online). Proton and neutron lifetimes for different baryon transfer models (cases I, II, and III) considered in Eqs. (12) and (52). The black line/gray regions show the lifetime range for any r, while blue curves correspond to particular r values.

More quantitatively, we compute $(\sigma v)_{\rm IND}$ using chiral perturbation theory, which provides an effective theory of baryons and mesons (and DM) from the underlying quark-level interaction in Eq. (52), following the same methods applied to standard nucleon decay [54] and with additional input from lattice calculations of hadronic matrix elements [55]. We refer the reader to Ref. [18] for further details. Figure 8 shows numerical results for the total cross section $(\sigma v)_{\rm IND}$, over the allowed mass range m_Ψ for $r = 1$, for the three types of interactions in Eq. (52).[12] This calculation agrees well with our previous estimate in Eq. (55). However, since the typical IND momentum is comparable to the chiral symmetry breaking scale ≈ 1 GeV (i.e., where the effective theory breaks down), we regard these results as approximate at best. The different rates for different cases (for fixed $\Lambda_{\rm IND}$) satisfy

$$(\sigma v)^{p\to K^+}_{\rm IND,III} = (\sigma v)^{n\to K^0}_{\rm IND,III}, \quad (\sigma v)^{p\to K^+}_{\rm IND,I} = (\sigma v)^{n\to K^0}_{\rm IND,II}, \quad (\sigma v)^{p\to K^+}_{\rm IND,II} = (\sigma v)^{n\to K^0}_{\rm IND,I}, \tag{57}$$

as a consequence of strong isospin symmetry [18]. The kinks correspond to up-scatting kinematic thresholds; to the left and right, only down-scatting is allowed, while in the center both up and down scattering occur.

More generally, we show in Fig. 9 the allowed range for $p \to K^+$ and $n \to K^0$ IND lifetimes. We consider masses $m_{\Psi,\Phi}$ consistent with $\Omega_{\rm DM}/\Omega_{\rm b} \approx 5$, for arbitrary r in the range $0 < r < \infty$, and we take $\Lambda_{\rm IND} = 1$ TeV. For case I (II), the allowed region is shown in gray, with a smaller (larger) lifetime for $n \to K^0$ than $p \to K^+$. For case III, shown by the black line, the p and n IND lifetimes are equal, modulo SUSY radiative corrections and isospin breaking that we neglect. Specific values for r are shown by blue curves. The solid blue curves show the IND lifetimes for $r = 1$, corresponding to the calculation in Fig. 8. For $r \neq 1$, the IND rate can be enhanced if the heavier state is overpopulated (e.g., $r > 1$ for $m_\Psi > m_\Phi$ or $r < 1$ for $m_\Psi < m_\Phi$); on the other hand, the IND rate can be highly suppressed if the heavier state is depleted and up scattering is kinematically forbidden. The dashed (dotted) blue curves show the IND lifetimes for $r = 5$ ($r = 1/5$).

We make a number of comments:

(i) The IND lifetimes scale as $\tau(N \to K) \propto \Lambda^6_{\rm IND}$. Taking $\Lambda_{\rm IND}$ in the range 500 GeV—5 TeV corresponds to lifetimes of 10^{30}–10^{36} yr. Lifetimes that

[12]The total rate $n \to K^0$ includes both K^0_S and K^0_L final states, and the individual channels $n \to K^0_S$ and $n \to K^0_L$ are (approximately) half the total rate.

can be probed in nucleon decay searches correspond to energy scales accessible in colliders (see below).

(ii) Both channels $p \to K^+$ and $n \to K^0$ provide complementary information, and which one dominates depends on the underlying heavy states mediating baryon transfer.

(iii) The largest IND rates in Fig. 9 correspond to Φ-dominated DM ($r \ll 1$) with $m_\Phi > m_\Psi$, and IND is dominated by $\Phi N \to \bar{\Psi} K$ down scattering.

Lastly, we note that while the observation of IND would be a smoking gun signal for hylogenesis, a nonobservation does not rule out hylogenesis as a baryogenesis mechanism. The IND rate can be suppressed if (i) the effective scale $\Lambda_{\rm IND}$ lies beyond the TeV scale (due to small couplings or large mass parameters), (ii) baryon transfer in the early universe involves heavier quark flavors, and/or (iii) the heavier DM state is depleted while up-scattering IND is kinematically blocked.

B. Precision probes

At energies well below the weak scale, the light states in the hidden sector interact with the SM primarily through the gauge kinetic mixing interaction. The most important effect of this mixing is an induced coupling of the Z' vector boson to the SM fermions f given by

$$-\mathcal{L} \supset -\kappa c_W Q_f^{em} \bar{f} \gamma^\mu Z'_\mu f, \tag{58}$$

where Q_f^{em} is the electric charge of the fermion and c_W is the cosine of the weak mixing angle. Direct searches for a light Z' limit $\kappa c_W \lesssim 10^{-3}$ for $m_{Z'} \lesssim 1$ GeV [33,34,56] with significant improvements expected in the coming years [57–59].

The dark matter states in our scenario consist of a Dirac fermion or a complex scalar with a direct coupling to the Z' vector. With the mixing interaction connecting the Z' to SM fermions, this state will efficiently mediate spin-independent elastic scattering of the DM states off nuclei. We estimate the cross section per target nucleon to be [16]

$$\sigma_0^{SI} = (5 \times 10^{-39}\ \text{cm}^2)\left(\frac{2Z}{A}\right)^2\left(\frac{\mu_n}{\text{GeV}}\right)^2\left(\frac{e'}{0.05}\right)^2 \times \left(\frac{\kappa}{10^{-4}}\right)^2\left(\frac{0.3\ \text{GeV}}{m_{Z'}}\right)^4, \tag{59}$$

where μ_n is the DM-nucleon reduced mass. While this cross section is quite large, the masses of the DM particles in this scenario lie below the region of sensitivity of most current direct detection DM searches, including the specific low-threshold analyses by COGENT [60], CDMS [61], XENON10 [62], and XENON100 [63]. For a DM mass below 3 GeV, this cross section lies slightly below the current best limit from CRESST [64]. Proposed low-threshold searches for DM scattering with nuclei or electrons are expected to improve these limits [65].

C. High-energy colliders

The new heavy states required for hylogenesis couple directly to the SM and can potentially be probed in high-energy colliders such as the Tevatron and the LHC. In particular, the effective interactions induced by the vector-like quark multiplets (P, P^c) can generate monojets and modify the kinematic distributions of dijets. We discuss here the approximate limits that existing collider data places on the masses of these multiplets, although we defer a detailed analysis to the future.

Monojet signals arising from the effective four-fermion interaction $(X u_R^c d_R^c s_R^c)/M^2$ present in the minimal hylogenesis model were considered previously in Ref. [18]. More recent searches for monojets by the ATLAS [66] and CMS [67] Collaborations limit the corresponding mass scale M to lie above 0.5–3 TeV. Note, however, that in our supersymmetric formulation the corresponding four-fermion operator is only generated once supersymmetry-breaking effects are included. This weakens the correlation between the monojet signal and the operator responsible for hylogenesis, although the limit does typically force the $P^{(c)}$ multiplets to be at least as heavy as a few hundred GeV. On the other hand, this operator is directly related to the IND interaction. An alternative signal that can arise directly from the superpotential interaction is a "monosquark" $\tilde{q}^* \tilde{X}$ final state, with the squark decaying to a jet and missing energy. In both cases, collider limits may be weakened through cascade decays in the hidden sector, which could produce additional hidden photons or Higgs bosons that decay to SM states.

A second way to probe our supersymmetric UV completion of hylogenesis is through the kinematic distributions of dijets, which can be modified by the direct production of the triplet P scalars (which are R even). On-shell production of scalar $\tilde{P}$ states via the interactions of Eq. (12) can produce a dijet resonance. For heavier masses, the primary effect is described by the nonminimal Kähler potential operator of Eq. (13), which gives rise to a four-quark contact operator. Studies of dijet distributions by ATLAS [68] and CMS [69,70] put limits on the masses of the $P^{(c)}$ scalars of 1–10 TeV, although the specific limits depend on the flavor structure of the quark coupling in Eq. (12) present in the underlying theory.

VI. CONCLUSIONS

Through the mechanism of hylogenesis, the cosmological densities of visible and dark matter may share a unified origin. Out-of-equilibrium decays during a low-temperature reheating epoch generate the visible baryon asymmetry, and an equal antibaryon asymmetry among GeV-scale hidden sector states. The hidden antibaryons are weakly coupled to the SM and are the dark matter in the Universe.

We have embedded hylogenesis in a supersymmetric framework. By virtue of its weak couplings to the SM,

SUSY-breaking is sequestered from the hidden sector, thereby stabilizing its GeV mass scale. The DM consists of two states, a quasidegenerate scalar-fermion pair of superpartners. We studied in detail one particular realization of supersymmetric hylogenesis, considering several aspects:

(i) We constructed a minimal supersymmetric model for hylogenesis. Hidden sector baryons are chiral superfields X and Y, with $B = 1$ and $-1/2$, respectively. The lightest Y states are DM, while X decays in the early universe generate the B asymmetries.

(ii) In addition, we introduced a vector-like $SU(3)_C$ triplet to mediate B transfer between visible and hidden sectors, and a hidden Z' gauge boson (with kinetic mixing) to deplete efficiently the symmetric DM densities.

(iii) We showed that hylogenesis can successfully generate the observed B asymmetry during reheating. We computed the CP asymmetry from X decay and solved the coupled Boltzmann equations describing the cosmological dynamics of hylogenesis.

(iv) We studied how SUSY breaking is communicated between the visible and hidden sectors through RG effects. We also examined predictions within an AMSB framework. While anomaly mediation explains the late-time reheating epoch from moduli decay, we have not explicitly addressed the issues of tachyonic slepton masses in the visible sector and the origin of SUSY mass terms in the hidden sector.

(v) Antibaryonic DM annihilates visible nucleons, causing induced nucleon decay to kaon final states, with effective nucleon lifetime in the range 10^{30}–10^{36} yr. DM can be discovered in current nucleon decay searches, and this signal remains unexplored.

(vi) Collider searches for monojets and dijet resonances provide the strongest direct constraints on our model, and these signals are correlated with IND. Lifetimes of 10^{30}–10^{36} years correspond to energy scales $\Lambda_{\rm IND} \sim 0.5$–$5$ TeV that can be probed at the LHC.

(vii) DM direct detection experiments and precision searches for hidden photons constrain the Z' kinetic mixing, although our model remains consistent with current bounds.

We emphasize that our specific model was constructed to illustrate general features of hylogenesis, and certainly there are many other model-building possibilities along these lines. Nevertheless, it is clear that supersymmetric hylogenesis provides a technically natural and viable scenario for the genesis of matter, explaining the cosmic coincidence between the dark and visible matter densities and predicting new experimental signatures to be explored in colliders and nucleon decay searches.

ACKNOWLEDGMENTS

We thank K. Zurek for helpful discussions. D. M. and K. S. would like to thank the Perimeter Institute for Theoretical Physics for their hospitality. The work of N. B., D. M., and K. S. is supported by the National Science and Engineering Research Council of Canada (NSERC). The work of S. T. was supported in part by the United States Department of Energy Grant No. DE-FG02-95ER40899 and by NSERC.

APPENDIX: ALTERNATE HIGGS PORTAL MODEL

We present here an alternate model for hylogenesis. In this model, hylogenesis cosmology is the same as described in Sec. III: a nonthermal abundance of X_1 states arises during a low temperature reheating epoch and decays out of equilibrium to produce equal-and-opposite baryon asymmetries in the visible and hidden sectors. The main difference, compared to the model in Sec. II, is that the symmetric DM particle-antiparticle density annihilates into light (GeV-scale) scalars, which in turn decay to SM fermions through mixing with the MSSM Higgs pseudoscalar A^0. We do not introduce a hidden sector $U(1)'$ gauge symmetry, and this allows for a reduced field content.

We suppose the hidden sector consists of (i) three vector-like chiral supermultiplets $X_{1,2}$ and Y, carrying $B = +1$ and $B = -1/2$, with charge-conjugate partners $X^c_{1,2}$ and Y^c, respectively, and (ii) a single $B = 0$ chiral supermultiplet N. The $X_{1,2}$ states are coupled to SM quarks via Eq. (11), and are responsible for generating CP asymmetries and B transfer between visible and hidden sectors, as in Sec. II. The hidden sector superpotential is

$$W_{\rm HS} = \zeta_a X_a Y^2 + \varepsilon N H_u H_d + \xi N Y Y^c + \frac{k}{3} N^3 + \mu_{X_a} X_a X^c_a, \tag{A1}$$

with couplings $\zeta_{1,2}$, ε, ξ, k, and where $H_{u,d}$ are the usual MSSM Higgs supermultiplets. Additional terms are forbidden by introducing a global $\mathbb{Z}_3$ symmetry under which N and Y^c carry opposite charge, while other fields are neutral. Since NH_uH_d breaks this symmetry explicitly, we take $\varepsilon \ll 1$. The soft SUSY-breaking terms are

$$-\mathcal{L}_{\rm soft} \supset m_N^2 |N|^2 + m_{\tilde{Y}}^2 |\tilde{Y}|^2 + m_{\tilde{Y}^c}^2 |\tilde{Y}^c|^2 + (A_k N^3 + A_\varepsilon N H_u H_d + A_\xi N \tilde{Y} \tilde{Y}^c + \text{H.c.}). \tag{A2}$$

We assume all couplings are real, and take $m_N^2 < 0$ such that the scalar component of N acquires a vev $\langle N \rangle \equiv \nu$, which generates mass terms for the DM states.

The physical spectrum of the hidden sector is given as follows. From the (Y, Y^c) supermultiplet pair, we have a Dirac fermion $\Psi \equiv (Y, Y^{c\dagger})$, with mass $m_\Psi = |\xi \nu|$, and two scalar states $\tilde{Y}$, $\tilde{Y}^c$, described by the mass matrix

$$\mathcal{L}_{\rm mass} = -(\tilde{Y}^\dagger, \tilde{Y}^c)\begin{pmatrix} m_{\tilde{Y}}^2 + m_\Psi^2 & \xi k\nu^2 + A_\xi \nu \\ \xi k\nu^2 + A_\xi \nu & m_{\tilde{Y}^c}^2 + m_\Psi^2 \end{pmatrix}\begin{pmatrix} \tilde{Y} \\ \tilde{Y}^{c\dagger} \end{pmatrix}. \tag{A3}$$

The mass eigenstates are given by $\Phi_{1,2}$, with masses

$$m_{\Phi_{1,2}}^2 = \frac{1}{2}(2m_\Psi^2 + m_{\tilde{Y}}^2 + m_{\tilde{Y}^c}^2 \pm \sqrt{(m_{\tilde{Y}}^2 - m_{\tilde{Y}^c}^2)^2 + 4(\xi k\nu^2 + A_\xi \nu)^2}), \tag{A4}$$

defined such that $m_{\Phi_1}^2 < m_{\Phi_2}^2$. DM consists of the states Ψ and Φ_1. For suppressed soft masses ($m_{\tilde{Y},\tilde{Y}^c}^2 \ll m_\Psi^2$), mixing is maximal (the relevant mixing angle is $\theta \approx \pi/4$) and $m_{\Phi_1} < m_\Psi < m_{\Phi_2}$.

The spectrum of N states consists of a real scalar s, pseudoscalar a, and Majorana fermion $\tilde{N}$. In the limit $\varepsilon \ll 1$, the leading $\mathcal{O}(\varepsilon)$ effects will be mixing between these states and the MSSM Higgs bosons and Higgsinos. Here, we set $\varepsilon = 0$, obtaining

$$m_s^2 = 4k^2\nu^2 + A_k\nu, \quad m_a^2 = -3A_k\nu, \quad m_{\tilde{N}}^2 = 4k^2\nu^2, \tag{A5}$$

where the soft mass m_N^2 has been traded for ν using the minimization condition. Vacuum stabilility requires $m_{s,a}^2 > 0$. These relations can be combined: $m_{\tilde{N}}^2 = m_s^2 + \frac{1}{3}m_a^2$.

A light pseudoscalar ($m_a < m_\Psi$, m_{Φ_1}) can provide an efficient channel for DM annihilation $\Psi\bar{\Psi} \to aa$ and $\Phi_1\Phi_1^\dagger \to aa$, with cross sections $\langle\sigma v\rangle \gtrsim 3\times 10^{-26}\,{\rm cm}^3/{\rm s}$ required to deplete the symmetric DM densities. For Φ_1 annihilation, the interaction $\mathcal{L} \supset -\frac{\xi^2}{2}a^2|\Phi_1|^2$ gives

$$\langle\sigma v\rangle_{\Phi_1\Phi_1^\dagger\to aa} = \frac{\xi^4}{256\pi m_{\Phi_1}^2}\sqrt{1 - m_a^2/m_{\Phi_1}^2} \approx 4\times 10^{-25}\ {\rm cm}^3/{\rm s} \times \left(\frac{\xi}{0.1}\right)^4\left(\frac{m_{\Phi_1}}{2\ {\rm GeV}}\right)^{-2}. \tag{A6}$$

For Ψ annihilation, t-channel $\Psi\bar{\Psi} \to aa$ is p-wave suppressed; however, if s is not too heavy ($m_s \lesssim 20$ GeV), it can mediate efficient s-channel annihilation:

$$\langle\sigma v\rangle_{\Psi\bar{\Psi}\to aa} = \frac{\xi^2(A_k - 2k^2\nu)^2}{256\pi(m_s^2 - 4m_\Psi^2)^2}\sqrt{1 - m_a^2/m_\Psi^2} \approx \frac{\xi^4 m_{\tilde{S}}^4}{1024\pi m_\Psi^2(m_s^2 - 4m_\Psi^2)^2}, \tag{A7}$$

where the second step follows by using the mass relations given in Eq. (A5) and assuming $m_a \approx 0$. For $m_\Psi = 3$ GeV, $m_s = m_{\tilde{S}} = 10$ GeV, $\xi = 0.1$, we have $\langle\sigma v\rangle \approx 4\times 10^{-25}\ {\rm cm}^3/{\rm s}$. In both cases, as long as $\xi \gtrsim 0.1$, the cross sections can easily be large enough to deplete the symmetric densities.

Depletion of the heavier DM state, e.g., $\Psi\bar{\Psi} \to \Phi_1\Phi_1^\dagger$ for $m_{\Phi_1} < m_\Psi$, may occur through t-channel $\tilde{N}$ exchange. We require $m_{\tilde{N}} > m_{\Phi_1} + m_\Psi \sim 5$ GeV to allow for decays $\tilde{N} \to \Phi_1\bar{\Psi}$ (otherwise $\tilde{N}$ would be an additional stable DM component); however, $\tilde{N}$ cannot be too heavy since $m_{\tilde{N}} \approx m_s \lesssim 20$ GeV. For $m_{\tilde{S}} \gg m_\Psi - m_{\Phi_1}$, and neglecting terms that are p-wave suppressed, the leading contribution to this cross section is

$$\langle\sigma v\rangle = \frac{\xi^4\cos^2 2\theta}{64\pi m_{\tilde{S}}^2}\sqrt{1 - m_{\Phi_1}^2/m_\Psi^2}, \tag{A8}$$

where θ is the $\tilde{Y}$ mixing angle. For $m_\Psi = 3$ GeV, $m_{\Phi_1} = 2$ GeV, $m_{\tilde{S}} = 10$ GeV, $\xi = 0.1$, we have

$$\langle\sigma v\rangle \approx 4\times 10^{-26}\ {\rm cm}^3/{\rm s} \times \cos^2 2\theta. \tag{A9}$$

The cross section for depletion of the heavier DM component is suppressed for maximal mixing ($\theta \approx \pi/4$), corresponding to the case when $m_{\tilde{Y}}^2$, $m_{\tilde{Y}^c}^2 \ll m_\Psi^2$.

After DM annihilation, the pseudoscalar can decay to SM fermions via mixing with the MSSM pseudoscalar boson A^0 through the $\varepsilon N H_u H_d$ term. The decay rate is

$$\Gamma(a \to f\bar{f}) = \frac{N_c \sin^2\alpha m_f^2 m_a}{16\pi v^2}\sqrt{1 - 4m_f^2/m_a^2} \times \begin{cases} \cot^2\beta & f = u \\ \tan^2\beta & f = d, \ell, \end{cases} \tag{A10}$$

where the A^0-a mixing angle is $\alpha \approx -\varepsilon m_{\tilde{S}} v/(2m_{A^0}^2)$. To avoid BBN constraints, we want $\Gamma^{-1} \lesssim 1\ {\rm s} \approx 6\times 10^{-25}\ {\rm GeV}^{-1}$. For $a \to \mu\bar{\mu}$, we have

$$\Gamma(a \to \mu\bar{\mu}) \approx 7\times 10^{-9}\ {\rm GeV} \times \tan^2\beta \sin^2\alpha\left(\frac{m_a}{1\ {\rm GeV}}\right). \tag{A11}$$

The decay rate for $a \to s\bar{s}$ is faster by a factor $\mathcal{O}(3)$ if kinematically available.

[1] For reviews of baryon creation, see A. Riotto and M. Trodden, Annu. Rev. Nucl. Part. Sci. **49**, 35 (1999); M. Dine and A. Kusenko, Rev. Mod. Phys. **76**, 1 (2003); S. Davidson, E. Nardi, and Y. Nir, Phys. Rep. **466**, 105 (2008); M. Dine and A. Kusenko, Rev. Mod. Phys. **76**, 1 (2003).

[2] For reviews of dark matter, see G. Jungman, M. Kamionkowski, and K. Griest, Phys. Rep. **267**, 195 (1996); G. Bertone, D. Hooper, and J. Silk, Phys. Rep. **405**, 279 (2005); G. D'Amico, M. Kamionkowski, and K. Sigurdson, arXiv:0907.1912.

[3] E. Komatsu *et al.* (WMAP Collaboration), Astrophys. J. Suppl. Ser. **192**, 18 (2011).

[4] S. Nussinov, Phys. Lett. **165B**, 55 (1985); S. M. Barr, R. S. Chivukula, and E. Farhi, Phys. Lett. B **241**, 387 (1990); S. M. Barr, Phys. Rev. D **44**, 3062 (1991); D. B. Kaplan, Phys. Rev. Lett. **68**, 741 (1992); D. E. Kaplan, M. A. Luty, and K. M. Zurek, Phys. Rev. D **79**, 115016 (2009); G. D. Kribs, T. S. Roy, J. Terning, and K. M. Zurek, Phys. Rev. D **81**, 095001 (2010); T. Cohen, D. J. Phalen, A. Pierce, and K. M. Zurek, Phys. Rev. D **82**, 056001 (2010).

[5] D. Hooper, J. March-Russell, and S. M. West, Phys. Lett. B **605**, 228 (2005).

[6] R. Kitano and I. Low, Phys. Rev. D **71**, 023510 (2005); R. Kitano and I. Low, arXiv:hep-ph/0503112.

[7] K. Agashe and G. Servant, J. Cosmol. Astropart. Phys. 02 (2005) 002.

[8] G. R. Farrar and G. Zaharijas, Phys. Rev. Lett. **96**, 041302 (2006).

[9] K. Kohri, A. Mazumdar, N. Sahu, and P. Stephens, Phys. Rev. D **80**, 061302 (2009).

[10] J. Shelton and K. M. Zurek, Phys. Rev. D **82**, 123512 (2010); N. Haba and S. Matsumoto, Prog. Theor. Phys. **125**, 1311 (2011); M. R. Buckley and L. Randall, J. High Energy Phys. 09 (2011) 009; E. J. Chun, Phys. Rev. D **83**, 053004 (2011); J. McDonald, Phys. Rev. D **83**, 083509 (2011); M. Blennow, B. Dasgupta, E. Fernandez-Martinez, and N. Rius, J. High Energy Phys. 03 (2011) 014; L. J. Hall, J. March-Russell, and S. M. West, arXiv:1010.0245; B. Dutta and J. Kumar, Phys. Lett. B **699**, 364 (2011); A. Falkowski, J. T. Ruderman, and T. Volansky, J. High Energy Phys. 05 (2011) 106; E. J. Chun, J. High Energy Phys. 03 (2011) 098; Z. Kang, J. Li, T. Li, T. Liu, and J. Yang, arXiv:1102.5644; J. J. Heckman and S.-J. Rey, J. High Energy Phys. 06 (2011) 120; D. E. Kaplan, G. Z. Krnjaic, K. R. Rehermann, and C. M. Wells, J. Cosmol. Astropart. Phys. 10 (2011) 011; M. T. Frandsen, S. Sarkar, and K. Schmidt-Hoberg, Phys. Rev. D **84**, 051703 (2011); A. Hook, Phys. Rev. D **84**, 055003 (2011); N. F. Bell, K. Petraki, I. M. Shoemaker, and R. R. Volkas, Phys. Rev. D **84**, 123505 (2011); C. Cheung and K. M. Zurek, Phys. Rev. D **84**, 035007 (2011); C. Arina and N. Sahu, Nucl. Phys. **B854**, 666 (2012); M. Y. Khlopov, Pis'ma Zh. Eksp. Teor. Fiz. **83**, 3 (2006) [JETP Lett. **83**, 1 (2006)].

[11] P. Hut and K. A. Olive, Phys. Lett. **87B**, 144 (1979).

[12] S. Dodelson and L. M. Widrow, Phys. Rev. D **42**, 326 (1990).

[13] V. A. Kuzmin, Phys. Part. Nucl. **29**, 257 (1998).

[14] P.-H. Gu, Phys. Lett. B **657**, 103 (2007); P.-H. Gu, U. Sarkar, and X. Zhang, Phys. Rev. D **80**, 076003 (2009); P.-H. Gu, M. Lindner, U. Sarkar, and X. Zhang, arXiv:1009.2690.

[15] H. An, S.-L. Chen, R. N. Mohapatra, and Y. Zhang, J. High Energy Phys. 03 (2010) 124; H. An, S.-L. Chen, R. N. Mohapatra, S. Nussinov, and Y. Zhang, Phys. Rev. D **82**, 023533 (2010).

[16] H. Davoudiasl, D. E. Morrissey, K. Sigurdson, and S. Tulin, Phys. Rev. Lett. **105**, 211304 (2010).

[17] H. Davoudiasl and R. N. Mohapatra, arXiv:1203.1247.

[18] H. Davoudiasl, D. E. Morrissey, K. Sigurdson, and S. Tulin, Phys. Rev. D **84**, 096008 (2011).

[19] For other applications of the $Xu_R d_R d_R$ operator to baryogenesis, see S. Dimopoulos and L. J. Hall, Phys. Lett. B **196**, 135 (1987); J. M. Cline and S. Raby, Phys. Rev. D **43**, 1781 (1991); S. D. Thomas, Phys. Lett. B **356**, 256 (1995); R. Kitano, H. Murayama, and M. Ratz, Phys. Lett. B **669**, 145 (2008); R. Allahverdi, B. Dutta, and K. Sinha, Phys. Rev. D **83**, 083502 (2011).

[20] T. Moroi and L. Randall, Nucl. Phys. **B570**, 455 (2000).

[21] K. Kobayashi *et al.* (Super-Kamiokande Collaboration), Phys. Rev. D **72**, 052007 (2005).

[22] T. Akiri *et al.* (LBNE Collaboration), arXiv:1110.6249.

[23] R. Abbasi *et al.* (IceCube Collaboration), arXiv:1111.2742.

[24] J. L. Hewett, H. Weerts, R. Brock, J. N. Butler, B. C. K. Casey, J. Collar, A. de Govea, and R. Essig *et al.*, arXiv:1205.2671.

[25] T. Cohen and K. M. Zurek, Phys. Rev. Lett. **104**, 101301 (2010).

[26] M. R. Buckley and S. Profumo, Phys. Rev. Lett. **108**, 011301 (2012).

[27] M. Cirelli, P. Panci, G. Servant, and G. Zaharijas, J. Cosmol. Astropart. Phys. 03 (2012) 015.

[28] S. Tulin, H.-B. Yu, and K. M. Zurek, arXiv:1202.0283.

[29] L. E. Ibanez and G. G. Ross, Phys. Lett. B **260**, 291 (1991).

[30] L. M. Krauss and F. Wilczek, Phys. Rev. Lett. **62**, 1221 (1989).

[31] M. Dine, L. Randall, and S. D. Thomas, Phys. Rev. Lett. **75**, 398 (1995).

[32] M. Pospelov, A. Ritz, and M. B. Voloshin, Phys. Lett. B **662**, 53 (2008).

[33] M. Pospelov, Phys. Rev. D **80**, 095002 (2009).

[34] J. D. Bjorken, R. Essig, P. Schuster, and N. Toro, Phys. Rev. D **80**, 075018 (2009).

[35] B. Batell, M. Pospelov, and A. Ritz, Phys. Rev. D **79**, 115008 (2009).

[36] Y. F. Chan, M. Low, D. E. Morrissey, and A. P. Spray, J. High Energy Phys. 05 (2012) 155.

[37] M. L. Graesser, I. M. Shoemaker, and L. Vecchi, arXiv:1103.277; H. Iminniyaz, M. Drees, and X. Chen, arXiv:1104.5548.

[38] R. Allahverdi, B. Dutta, and K. Sinha, Phys. Rev. D **82**, 035004 (2010).

[39] B. S. Acharya, G. Kane, and E. Kuflik, arXiv:1006.3272.

[40] D. J. H. Chung, E. W. Kolb, and A. Riotto, Phys. Rev. D **60**, 063504 (1999).

[41] G. F. Giudice, E. W. Kolb, and A. Riotto, Phys. Rev. D **64**, 023508 (2001).

[42] T. Lin, H.-B. Yu, and K. M. Zurek, Phys. Rev. D **85**, 063503 (2012).

[43] U. Ellwanger and P. Mitropoulos, J. Cosmol. Astropart. Phys. 07 (2012) 024.
[44] M. Baumgart, C. Cheung, J. T. Ruderman, L.-T. Wang, and I. Yavin, J. High Energy Phys. 04 (2009) 014.
[45] D. E. Morrissey, D. Poland, and K. M. Zurek, J. High Energy Phys. 07 (2009) 050.
[46] A. Kumar, D. E. Morrissey, and A. Spray, J. High Energy Phys. 12 (2011) 013.
[47] S. Kachru, R. Kallosh, A. D. Linde, and S. P. Trivedi, Phys. Rev. D **68**, 046005 (2003); R. Kallosh and A. D. Linde, J. High Energy Phys. 02 (2007) 002.
[48] J. Fan, M. Reece, and L.-T. Wang, J. High Energy Phys. 09 (2011) 126.
[49] L. Randall and R. Sundrum, Nucl. Phys. **B557**, 79 (1999).
[50] G. F. Giudice, M. A. Luty, H. Murayama, and R. Rattazzi, J. High Energy Phys. 12 (1998) 027.
[51] J. L. Feng, V. Rentala, and Z. Surujon, Phys. Rev. D **84**, 095033 (2011); J. L. Feng, V. Rentala, and Z. Surujon, Phys. Rev. D **85**, 055003 (2012).
[52] A. Pomarol and R. Rattazzi, J. High Energy Phys. 05 (1999) 013.
[53] Z. Chacko, M. A. Luty, I. Maksymyk, and E. Ponton, J. High Energy Phys. 04 (2000) 001.
[54] M. Claudson, M. B. Wise, and L. J. Hall, Nucl. Phys. **B195**, 297 (1982).
[55] Y. Aoki, P. Boyle, P. Cooney, L. Del Debbio, R. Kenway, C. Maynard, A. Soni, and R. Tweedie (RBC-UKQCD Collaboration), Phys. Rev. D **78**, 054505 (2008).
[56] M. Reece and L.-T. Wang, J. High Energy Phys. 07 (2009) 051.
[57] H. Merkel *et al.* (A1 Collaboration), Phys. Rev. Lett. **106**, 251802 (2011).
[58] S. Abrahamyan *et al.* (APEX Collaboration), Phys. Rev. Lett. **107**, 191804 (2011).
[59] S. Andreas and A. Ringwald, arXiv:1008.4519.
[60] C. E. Aalseth *et al.* (CoGeNT Collaboration), Phys. Rev. Lett. **106**, 131301 (2011).
[61] D. S. Akerib *et al.* (CDMS Collaboration), Phys. Rev. D **82**, 122004 (2010); Z. Ahmed *et al.* (CDMS-II Collaboration), Phys. Rev. Lett. **106**, 131302 (2011).
[62] J. Angle *et al.* (XENON10 Collaboration), Phys. Rev. Lett. **107**, 051301 (2011).
[63] E. Aprile *et al.* (XENON100 Collaboration), Phys. Rev. Lett. **107**, 131302 (2011).
[64] G. Angloher *et al.*, Astropart. Phys. **18**, 43 (2002).
[65] R. Essig, J. Mardon, and T. Volansky, Phys. Rev. D **85**, 076007 (2012).
[66] ATLAS Collaboration, Report No. ATLAS-CONF-2011-096, 2012.
[67] T. Aaltonen *et al.* (CDF Collaboration), arXiv:1203.0742.
[68] ATLAS Collaboration, Report No. ATLAS-CONF-2012-038, 2012.
[69] S. Chatrchyan *et al.* (CMS Collaboration), J. High Energy Phys. 05 (2012) 055.
[70] S. Chatrchyan *et al.* (CMS Collaboration), Phys. Lett. B **704**, 123 (2011).